



Weathering geochemistry and Sr-Nd fingerprints of equatorial upper Nile and Congo muds

Eduardo Garzanti, Marta Padoan, and Luigi Peruta

Laboratory for Provenance Studies, Department of Earth and Environmental Sciences, Università di Milano-Bicocca, Milano, Italy (eduardo.garzanti@unimib.it)

Massimo Setti

Dipartimento di Scienze della Terra e dell' Ambiente, Università di Pavia, Pavia, Italy

Yani Najman

Department of Environmental Science, Lancaster University, Lancaster, UK

Igor M. Villa

Laboratory for Provenance Studies, Department of Earth and Environmental Sciences, Università di Milano-Bicocca, Milano, Italy

Institut für Geologie, Universität Bern, Baltzerstrasse 3, Bern, Switzerland

[1] This study investigates processes of sediment generation in equatorial central Africa. An original, complete and integrated mineralogical-geochemical database on silt-sized sediments derived from different parent rocks (basalt, granite, gneiss, metapsammite, sandstone) along the East African Rift from 5°S in Tanzania to 5°N in Sudan is presented and used to assess the incidence of diverse factors controlling sediment composition (source-rock lithology, geomorphology, hydraulic sorting, grain size, recycling), with particular emphasis on chemical weathering.

Components: 16,200 words, 9 figures, 2 tables.

Keywords: clay minerals; chemical weathering indices; model mantle derivation ages; recycling; Kagera catchment; East African Rift.

Index Terms: 3675 Mineralogy and Petrology: Sedimentary Petrology; 8175 Tectonophysics: Tectonics and Landscape Evolution; 9305 Geographic Location: Africa.

Received 3 July 2012; **Revised** 20 December 2012; **Accepted** 27 December 2012; **Published** 21 February 2013.

Garzanti E., M. Padoan, M. Setti, Y. Najman, L. Peruta, and I. M. Villa (2013), Weathering geochemistry and Sr-Nd fingerprints of equatorial upper Nile and Congo muds, *Geochem. Geophys. Geosyst.*, 14, 292–316, doi:10.1002/ggge.20060.

[2] Kaolinite abundance, CIA, and α^{Al} values consistently indicate less intense weathering along the steep inner flank and drier axis of the rift hosting Lakes Kivu and Tanganyika than in hot-humid forested highlands east of the Nile-Congo divide, where slopes are gentler and time for weathering longer. The

observed order of bulk-sediment mobility ($Na \geq Ca > Sr > Mg > K > Ba \geq Rb > Cs$) roughly corresponds to the degree into which these elements are partitioned into unstable plagioclase versus K-feldspar and phyllosilicates. Weathering-limited erosion characterizes the Rwenzori massif and the Lake Albert

graben where sediments are recycled from syn-rift deposits. $^{87}\text{Sr}/^{86}\text{Sr}$ ratios, $^{143}\text{Nd}/^{144}\text{Nd}$ ratios, and Sm-Nd t_{DM} model ages of river muds proved instead to be insensitive to weathering and provided a faithful integrated signature of the geology of each drainage basin.

[3] The comparison of CIA and WIP indices offers a key for discriminating compositional modifications due to weathering and recycling, a most challenging problem in sedimentary geochemistry. Integrated mineralogical-geochemical databases are essential to improve our understanding of weathering processes as they occur in the natural environment and to distinguish their effect from other factors controlling sediment composition.

“When the sun goes down over Kigali, if you still have the remains of a soul, you cannot do otherwise than stop talking and watch.”

Gil Courtemanche, *A Sunday at the Pool in Kigali*

1. Introduction

[4] The East African Rift supplies water and sediments to the Nile and Congo Rivers, two of the largest drainage systems on Earth. This equatorial region, where hot and humid climate leads to a maximum of chemical weathering, is an excellent natural laboratory in which to study the products of denudation of continental crust at the core of the African continent. The mineralogical, chemical, and isotopic signatures of sediments produced in this region can be used to investigate the various factors controlling sediment composition and specifically how and to what extent the fingerprints of different parent-rock lithologies are modified by weathering at the source prior to entering the routing system and subsequently by both physical and chemical processes during multistep transport and deposition [Martin and Meybeck, 1979; Velbel, 1993; Edmond et al., 1996; Nesbitt et al., 1996; Canfield, 1997; Moquet et al., 2011; Lupker et al., 2012]. Another crucial aspect addressed here is the identification of criteria to differentiate weathered first-cycle versus polycyclic sediments [Johnsson, 1993; Gaillardet et al., 1999].

[5] Information on the geochemistry of river sediments of various grain sizes from central Africa are still limited [Martin et al., 1978; Négrel et al., 1993; Dupré et al., 1996; Viers et al., 2009], and very little is known from the headwaters of the Nile and Congo Rivers. This article, presenting detailed integrated mineralogical-geochemical information on river muds of equatorial Africa, is companion

to mineralogical and petrological studies of river sands in the same region [Andò et al., 2012; Garzanti et al., in review] and follows a similar work carried out on the White and Blue Nile in Sudan and Ethiopia [Padoan et al., 2011].

2. The East African Rift

[6] In this section, we briefly outline the main geological and geomorphological features of the study area. Specific reference is made to the distinctive isotopic signatures of diverse parent rocks, which in the following sections will be compared to those characterizing fluvial sediments, in order to determine their susceptibility to weathering and to assess the relative sediment contributions from different sources in various catchments.

2.1. Geological Framework

[7] The study area follows the western branch of the East African Rift [Ebinger, 1989] and straddles the equatorial belt, from a latitude of $\text{S}5^{\circ}13'$ in NW Tanzania to a latitude of $\text{N}4^{\circ}51'$ in South Sudan (Figure 1). Uplifted along the rift shoulders since the Miocene are low to high-grade metamorphic rocks formed during successive Archean to Proterozoic orogenic events (Figure 2). Widely exposed in northern Uganda are largely Mesoarchean epidote-amphibolite to granulite-facies gneisses (Gneissic-Granulitic Complex) [Schlüter, 2008]. Paleoproterozoic basements are represented by low-grade schists to amphibolite-facies gneisses and granitoids of the Buganda-Toro belt [Nagudi et al., 2003], exposed from Lake Victoria in the east to the Rwenzori horst in the west, and by remnants of the Rusizian-Ubendian belt [Link et al., 2010]. These include garnet-biotite-sillimanite gneisses, migmatites, quartzites, and granitoids exposed along the eastern shoulder of Lakes Kivu and Tanganyika [Fernandez-Alonso and Theunissen, 1998].

[8] The Mesoproterozoic Karagwe-Ankole Belt, exposed across Burundi and Rwanda, consists of mainly low-grade meta-sediments intruded by igneous rocks (Western Domain), overthrust on less deformed strata resting on the Tanzania Craton in the south (Eastern Domain) [Fernandez-Alonso, 2007; Tack et al., 2010]. Widespread granitoids and localized mafic-ultramafic layered intrusions dated at 1.38–1.37 Ga [Duchesne et al., 2004; Maier et al., 2008] were followed by alkali granites and pegmatites emplaced in shear zones, and finally at 0.99–0.97 Ga by tin granites associated with Sn, W, Nb, and Ta mineralizations [Klerkx et al., 1987;

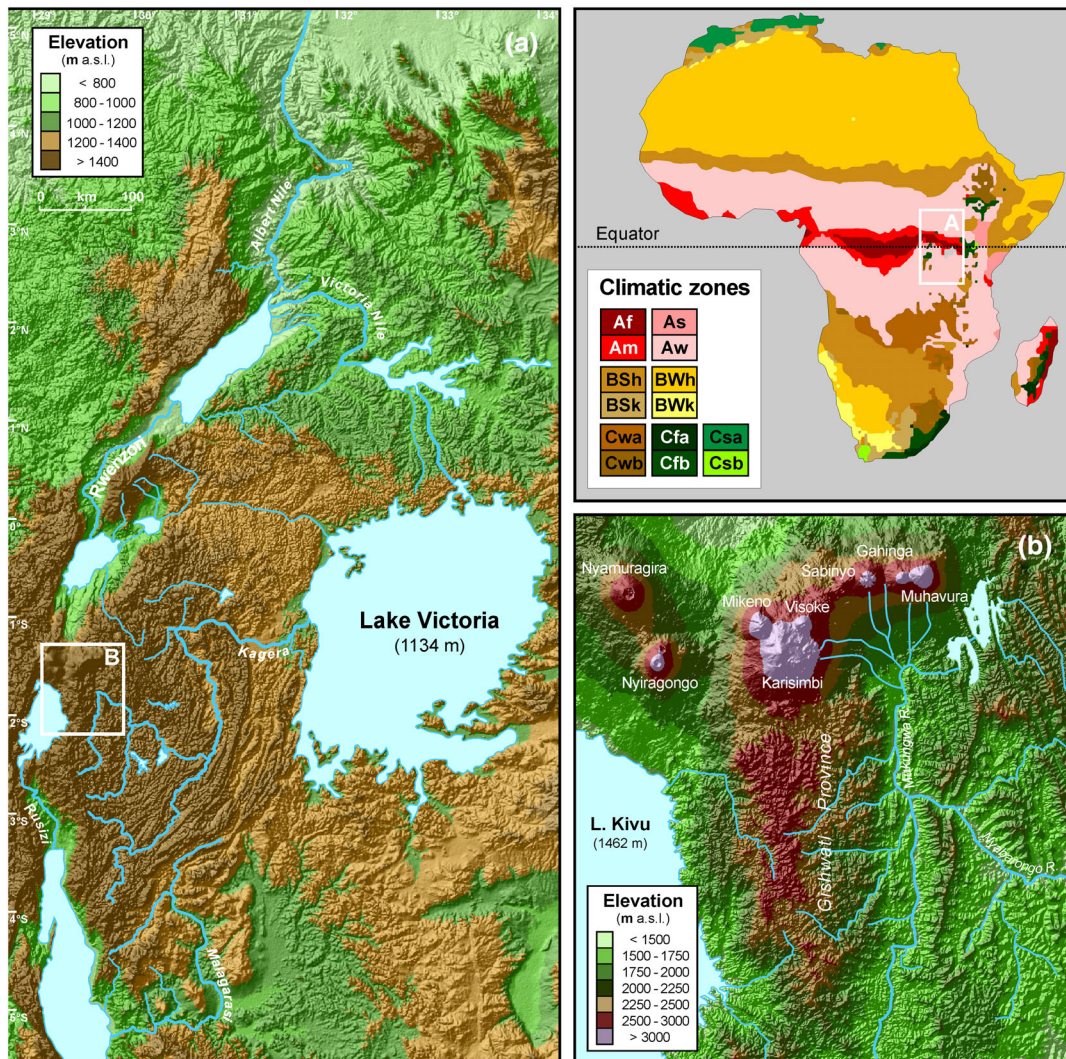


Figure 1. Climate and relief in equatorial Africa. (a) Topography and drainage patterns in the study area. (b) Virunga volcanic field and Gishwati Province (northern part of the Tanganyika-Kivu rift shoulder). Shown in the upper right panel is the distribution of climatic zones (Köppen-Geiger classification after Kottek *et al.* [2006]). *Main climates:* A = equatorial; B = arid; C = warm temperate. *Precipitation:* W = desert; S = steppe; f = fully humid; s = summer dry; w = winter dry; m = monsoonal. *Temperature:* h = hot arid; k = cold arid; a = hot summer; b = warm summer.

Pohl, 1994]. The tightly folded and several kilometer thick stratigraphic succession of the Western Domain consists of dark phyllites intercalated with quartzites, meta-conglomerates and basaltic to rhyolitic sills and lavas, followed by metasandstones and metapelites with rare dolostone lenses and cherty mudrocks at the top (Akanyaru Supergroup) [Baudet *et al.*, 1988; Fernandez-Alonso *et al.*, 2012]. The less deformed stratigraphic succession of the Eastern Domain straddles the Tanzania/Burundi boundary as far as Lake Victoria (Kagera Supergroup), whereas to the south in NW Tanzania, sub-tabular sandstones with subordinate mudrocks, conglomerates, dolostones, and chert are intercalated with thick Neoproterozoic basaltic lavas (Malagarasi Supergroup)

[Deblond *et al.*, 2001]. Neoproterozoic intrusive and metamorphic events are revealed, respectively, in Burundi by the Upper Ruvubu alkaline complex mainly including feldspathoid-bearing syenites (~0.74 Ga) [Tack *et al.*, 1994] and in central Uganda by kyanite-garnet schists yielding U-Th-Pb monazite ages of 0.62–0.63 Ga at Murchison Falls [Appel *et al.*, 2005].

[9] Volcanism began at ~12 Ma, is restricted to three accommodation zones between extensional basins, and shows a northward increase in alkaline character and CO₂ content. Tholeiites and alkali basalts of the South Kivu field were produced by fault-related activity dominated by fissure eruptions [Furman and Graham, 1999]. Two active

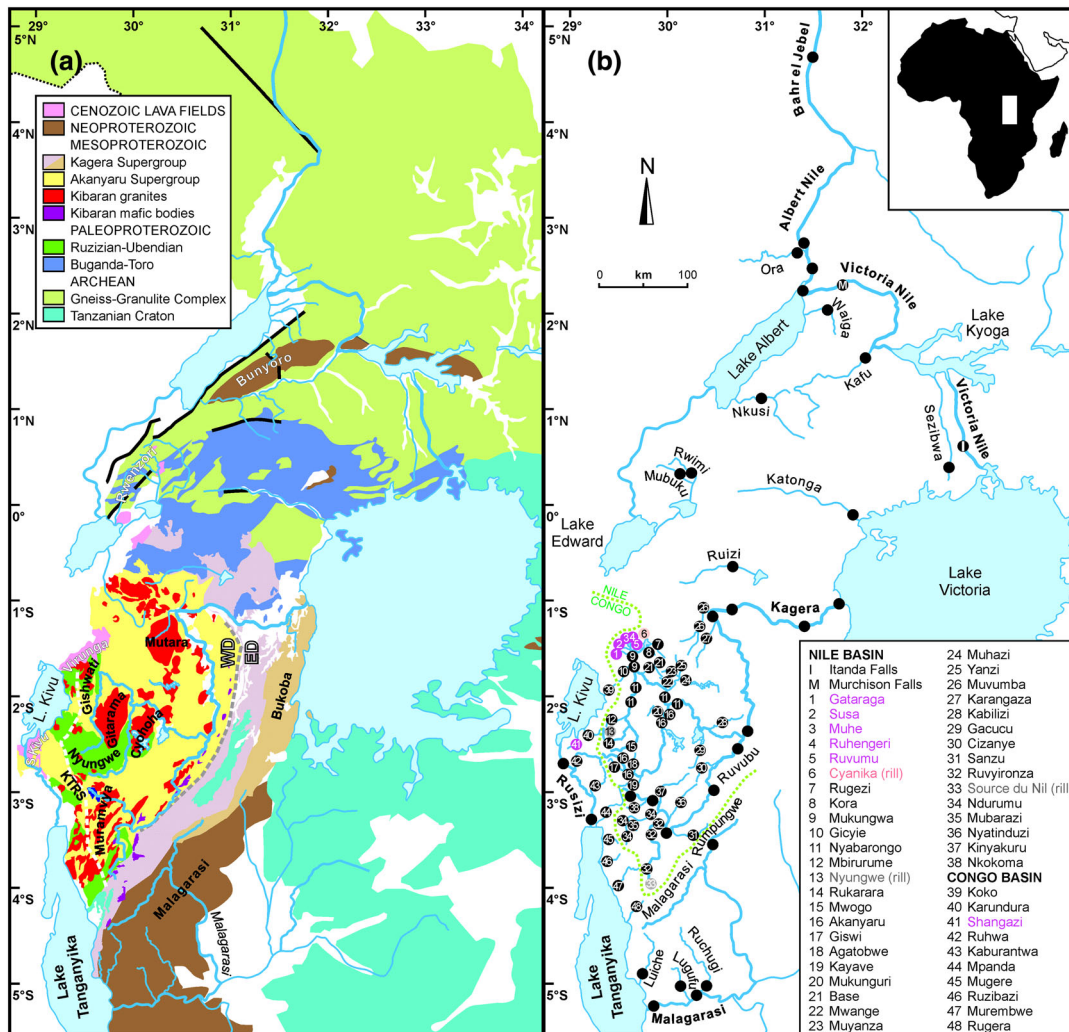


Figure 2. The western branch of the East African Rift with identified sedimentary provinces. (a) Geological sketch map (compiled after Schlüter [2008], Fernandez-Alonso [2007], and other sources cited in text). KTRs = Kivu-Tanganyika rift shoulder. WD, ED = Western and Eastern Domains [Tack et al., 2010]. (b) Studied rivers and sampling sites.

volcanoes and six extinct cones reaching up to 4507 m above sea level (asl) form the potassic Virunga field (Figure 1b), straddling the Rwanda-Uganda-Congo border and including K-basanites and K-hawaiites, and locally latites or K-trachytes [Ebinger and Furman, 2003]. The active Toro-Ankole field, aligned parallel to active faults east of the Rwenzori mountains, includes exceptionally silica-undersaturated melts and carbonatites [Rosenthal et al., 2009]. Rift-related basins are filled by Neogene fluvial to lacustrine sediments.

2.2. Previous Isotopic Data

[10] Isotopic studies have long been carried out on Neogene lavas [e.g., Holmes and Harwood, 1937; Bell and Powell, 1969]. More recent works reported

$^{87}\text{Sr}/^{86}\text{Sr}$ ratios of 0.704 ± 0.01 and $\epsilon\text{Nd}_{(0)}$ of 3 ± 2 in the South Kivu field [Furman and Graham, 1999], and $^{87}\text{Sr}/^{86}\text{Sr}$ ratios of 0.705 ± 0.01 and $\epsilon\text{Nd}_{(0)}$ of -2 ± 1 in the Toro-Ankole field [Rosenthal et al., 2009]. Values are more varied in the Virunga field, where $^{87}\text{Sr}/^{86}\text{Sr}$ ratios range from 0.706 in low-silica K-basanites to 0.710 in latites of the Sabinyo volcano showing evidence of lower-crustal contamination, and reach up to 0.713 in most evolved trachytic lavas of the Karisimbi volcano (Figure 1b); $\epsilon\text{Nd}_{(0)}$ ranges from -11 to -2 [Vollmer and Norry, 1983; De Mulder et al., 1986; Rogers et al., 1992]. The model age of ~ 1 Ga calculated for the mantle-lithosphere magma source is similar to that of most recent episodes of post-orogenic granite magmatism in the basement and may be explained by mixing

with silicic melts from deep Paleoproterozoic crust [Rogers *et al.*, 1998].

[11] In the mafic-ultramafic and granitic Kibaran intrusions studied so far, $^{87}\text{Sr}/^{86}\text{Sr}$ ratios are 0.710 ± 0.006 and 0.78 ± 0.02 , respectively, whereas $\epsilon\text{Nd}_{(0)}$ is -9 ± 6 and -16 ± 2 , respectively [Tack *et al.*, 1994; Duchesne *et al.*, 2004]. $^{87}\text{Sr}/^{86}\text{Sr}$ ratios may reach above 0.9 in post-Kibaran pegmatites and mineralized veins [Brinckmann *et al.*, 1994; Lehmann *et al.*, 1994]. Sm-Nd t_{DM} model ages for Kibaran mafic-ultramafic to granite intrusions mostly range from 0.9 to 2.5 Ga [Tack *et al.*, 1994; Duchesne *et al.*, 2004]. Four Mesoproterozoic granitoid bodies intruding low-grade Karagwe-Ankole meta-sediments in southernmost Uganda yielded more negative $\epsilon\text{Nd}_{(0)}$ between -20 and -35 , and older t_{DM} model ages between 3.8 and 2.9 Ga [Buchwaldt *et al.*, 2008].

[12] Information on gneissic basements is incomplete. One orthogneiss of the Rusizian basement (SHRIMP zircon U-Pb age 1986 ± 6 Ma) yielded a zircon Lu-Hf model age of 2.3 ± 0.1 Ga, suggesting participation of early Paleoproterozoic crust in its generation. Similar to slightly younger model ages are yielded by Kibaran granitoids and migmatitic paragneisses (2.1 ± 0.2 Ga) and younger tin granites (2.0 ± 0.3 Ga), indicating repeated re-melting of Rusizian basement during the Mesoproterozoic with limited addition of mantle-derived juvenile components [Tack *et al.*, 2010].

2.3. Geomorphology

[13] Because of rift-related doming, the region has considerable relief. The altitude of numerous lakes, representing local erosional base level, ranges from 619 m (Albert) and 773 m (Tanganyika) to 1134 m (Victoria) and 1462 m asl (Kivu), whereas the Rwenzori massif touches as high as 5110 m. The rift shoulder marking the drainage divide between the Nile and Congo Rivers from Burundi to Rwanda reaches between 2500 and 3000 m. West of this ridgeline, the land slopes abruptly toward Lakes Kivu and Tanganyika, joined along the rift axis by the Ruzizi River. The eastern slopes, drained by the four major branches of the Kagera River in Burundi (Ruvubu, Ruvyironza) and Rwanda (Nyabarongo, Akanyaru), are less steep, with rolling hills extending across the central-plateau uplands to the low hills and papyrus swamps grading into Lake Victoria (Figure 1).

[14] Average air temperatures, ranging from 15°C to 30°C with minor seasonal and diurnal variation, are

markedly influenced by altitude. Freezing nights characterize the rugged Rwenzori mountains, where the highest peaks are permanently covered by snowfields and small rapidly retreating glaciers [Ring, 2008; Taylor *et al.*, 2009]. Delivered during the passage of the inter-tropical convergence zone by humid masses blown by the southeasterly monsoon from the Indian Ocean, rainfall is distributed in two rainy seasons in autumn and spring. Annual precipitations range from ≤ 1 m along the eastern coast of Lake Tanganyika to 1.5 m along the northern coast of Lake Victoria, reaching up to 2 m on rift-shoulder reliefs across the Rwanda-Burundi border (Figure 3a). Peak flow in the Kagera basin ($60,000 \text{ km}^2$) occurs in April in the upper tributaries but is attenuated downstream by numerous lakes and swamps and consequently delayed to July in the lower course, where long-term mean annual runoff is only 136 mm compared with rainfall of 1170 mm [Sutcliffe and Parks, 1999]. Along eastern Rwenzori slopes, precipitations decrease sharply from 2.5 m on the mountains where rain or snow falls nearly every day (Rwenzori = “rain maker” in local language), to 0.75 m in the rain shadow at the foot of the range.

[15] Rain forests cover a small part of the territory in rift and volcanic highlands, and grade through sub-humid acacia woodland to more arid shrubland and grassland. Soil temperature and moisture regimes vary from udic isothermic/isomesic on Burundi and Rwanda highlands characterized by kaolinite-rich nitisols [Nizeyimana and Bicki, 1992; Soil map of Rwanda, 1994] to ustic iso-hyperthermic in savannah lowlands characterized by ferralsols (Figure 3b). Because of widespread development of thick red-brown ferrallitic soils and extensive vegetation cover, rock outcrops are scarce and limited to most resistant lithologies (e.g., quartzite and amphibolite) [Moeyersons, 2003]. Where exposed, Mesoproterozoic meta-sediments are generally transformed into saprolite; sparse hillocks remain as isolated witnesses of large granitoid intrusions.

3. Sampling and Methods

[16] Eighty-five samples of freshly deposited mud were collected in February 2007 and June 2008, along the banks of rivers draining the East African Rift. Mud in rills incising soil profiles developed on basaltic lavas, medium-grade gneisses, and low-grade meta-sediments were also collected at the source of diverse branches of the Kagera-Nile, in order to check weathering at the very beginning of the sediment-routing system. For major rivers,

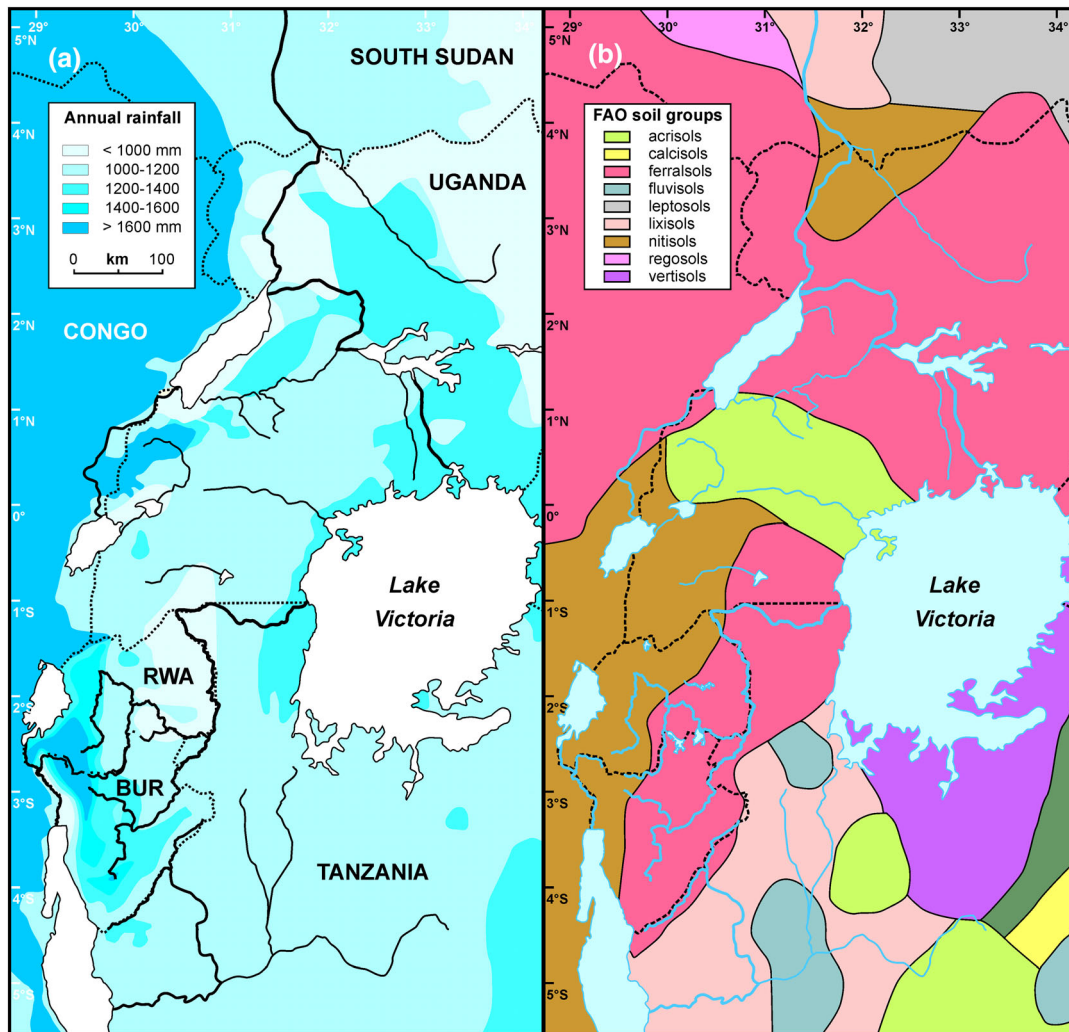


Figure 3. Climate and soil types in equatorial central Africa. (a) Rainfall map. (b) Soil map (distribution of soil groups as classified by the Food and Agriculture Organization, www.britannica.com/bps/media-view/19257/0/0/0). RWA = Rwanda; BUR = Burundi.

samples were collected upstream and well downstream of major confluences in order to monitor compositional changes caused by both tributary input and weathering in temporary-storage sites and swamps, with particular detail for the Kagera basin (Figure 2). The analyzed samples are mainly poorly sorted, coarse to very coarse silts (6 to 4ϕ), including variable percentages of sand ($30\pm 30\%$) and clay. Only Virunga muds lack clay. River mud, which is easy to sample compared to suspended sediments, is used in this study as a proxy of chemical weathering intensity and analyzed to understand its control.

3.1. Mineralogy

[17] The mineralogical composition of 41 mud samples was determined by X-ray powder diffraction (XRD) at the University of Pavia, using a Philips[®]

PW 1800 diffractometer with $\text{CuK}\alpha$ radiation. Deposited mud is a mixture of clay, silt, and very fine grained sand carried in suspension. Occasionally, some underlying or intercalated sandy layers may have been collected inadvertently during sampling, which would lead to biased analytical results (e.g., excess quartz). In order to check for and minimize such potential contamination effects, the analyses were carried out both on bulk samples and on the $< 63 \mu\text{m}$ fraction after eliminating sand by sieving. Relative mineral abundances were estimated from the height of the main peaks [Biscaye, 1965; Moore and Reynolds, 1989]. In the same samples, clay minerals were analyzed on the $< 2 \mu\text{m}$ fraction, separated by settling in a water column. Samples were mounted as oriented aggregates on glass slides. X-ray patterns were recorded in natural conditions (air dried), after ethylene glycol

solvatation. The identified minerals are listed in order of abundance through the text.

3.2. Geochemistry

[18] Geochemical analyses of the 70 samples collected in June 2008 were carried out at ACME Laboratories, Vancouver. In the 35 samples containing $\geq 10\%$ sand, the sand fraction was eliminated by sieving at $63 \mu\text{m}$; sand-poor samples were analyzed in bulk. Following a lithium metaborate/tetraborate fusion and nitric acid digestion, major oxides were determined by ICP-ES and trace elements by ICP-MS. A separate split was digested in aqua regia and analyzed by ICP-MS for Mo, Ni, Cu, Ag, Au, Zn, Cd, Hg, Tl, Pb, As, Sb, Bi, and Se; these elements may have been systematically underestimated because of only partial digestion particularly of refractory minerals. Discrepancies observed in replicate analyses, $\leq 1\%$ for major elements and $\leq 5\%$ for most trace elements, occasionally reach 15–25% for Be, Au, and S. Loss on ignition (LOI) is by weight difference after ignition at 1000°C , carbon and sulfur analysis by Leco (for further information on adopted procedures, geostandards used, and precision for various elements of group 4A–4B, see <http://acmelab.com>). Another 15 additional or replicate samples collected in February 2007 were analyzed by XRF at Open University.

[19] Chemical composition is discussed with reference to the estimated element concentration in the upper continental crust (UCC) and standard shale (PAAS) [Taylor and McLennan, 1985; 1995; McLennan, 2001; Hu and Gao, 2008]. REE data were normalized to CI carbonaceous chondrites [McDonough and Sun, 1995]. Among the numerous indices proposed to estimate chemical weathering, we considered specifically the Chemical Index of Alteration (CIA) [Nesbitt and Young, 1982] and the Weathering Index (WIP) [Parker, 1970], both calculated using molecular proportions of mobile alkali and alkaline-earth metals corrected for Ca in apatite (no correction for Ca in carbonates was required because all studied samples lack carbonates):

$$\text{CIA} = 100 * \text{Al}_2\text{O}_3 / (\text{Al}_2\text{O}_3 + \text{CaO} - 3.33 * \text{P}_2\text{O}_5 + \text{Na}_2\text{O} + \text{K}_2\text{O}) \quad (1)$$

$$\text{WIP} = 100 * [(\text{CaO} - 3.33 * \text{P}_2\text{O}_5) / 0.7 + 2\text{Na}_2\text{O} / 0.35 + 2\text{K}_2\text{O} / 0.25 + \text{MgO} / 0.9] \quad (2)$$

[20] Stronger weathering is indicated by higher CIA, widely interpreted as a measure of the extent of

conversion of feldspars to clays such as kaolinite, and by lower WIP, held to be appropriate for heterogeneous sources including metamorphic rocks [Price and Velbel, 2003; Borges and Huh, 2007; Shao et al., 2012]. Because it simply reflects concentrations of Mg, Ca, Na, and K, the WIP is markedly affected by quartz dilution and overestimates weathering in quartz-rich sediments. When comparing pairs of mud and sand samples, the WIP thus commonly results to be lower in the sand because it contains more quartz.

[21] Weathering intensities can also be calculated for each single element mobilized during incongruent weathering of silicates (Mg, Ca, Na, Sr, K, Ba) by comparing its concentration to that of a non-mobile element with similar magmatic compatibility (Al, Ti, Sm, Nd, Th) in our samples and in UCC (e.g., $\alpha_{\text{Ca}} = [\text{Ti}/\text{Ca}]_{\text{sample}} / [\text{Ti}/\text{Ca}]_{\text{UCC}}$) [Gaillardet et al., 1999]. The ratio to non-mobile elements minimizes the uncertainty that exists on the composition of crustal source rocks as well as the effect of quartz dilution and thus also partly of grain size and recycling. On the other hand, the non-mobile elements Th, Nd, Sm, and to a lesser extent Ti are preferentially hosted in dense and ultradense minerals (e.g., monazite, allanite, titanite, ilmenite, and rutile) that can be strongly concentrated locally by hydrodynamic processes. As a consequence, α values yield misleading results when used to assess weathering for samples displaying anomalous hydraulic concentration of dense detrital components [Garzanti et al., 2009]. Hydraulic-sorting bias can be effectively minimized by calculating weathering intensities with reference to non-mobile elements not concentrated equally strongly in ultradense minerals (e.g., Al). We thus defined α^{Al} values for any element E as

$$\alpha^{\text{Al}}_E = [\text{Al}/E]_{\text{sample}} / [\text{Al}/E]_{\text{UCC}} \quad (3)$$

and found that within each homogeneous province across equatorial Africa, the standard deviation of α^{Al} values is systematically lower (by factors ranging from 1.5–3 for $\alpha^{\text{Al}}_{\text{Ca}}$ to 3–5 or even more for $\alpha^{\text{Al}}_{\text{K}}$ and $\alpha^{\text{Al}}_{\text{Ba}}$) than that of α values as defined by Gaillardet et al. [1999]. The more consistent and reliable α^{Al} values as defined in equation (3) will thus be given throughout this article, and their use is recommended in any weathering study. It must be noted that although α^{Al} values do minimize hydraulic-sorting effects associated with settling equivalence and selective entrainment [Garzanti et al., 2008; 2010], they tend to emphasize the more subtle effects associated with suspension

sorting [Bouchez *et al.*, 2011a; Garzanti *et al.*, 2011]. In suspended load carried by the Amazon and Ganga-Brahmaputra Rivers [Bouchez *et al.*, 2011b; Lupker *et al.*, 2012], Na increases with water depth faster than Sr and Ca, whereas Nd, Sm, and Th tend to slightly decrease, and Cs, Rb, K, Be, and Ba decrease at slower rates than Mg, Ti, and Al. As a result, α_{Mg} is virtually invariant with depth, α_{Ca} and α_{Ca}^{Al} decrease at a similar rate, but α_{Sr}^{Al} and α_{Na}^{Al} decrease faster than α_{Sr} and α_{Na} , and α_{Ba}^{Al} and α_{K}^{Al} tend to decrease whereas α_{Ba} and α_{K} tend to increase. Such discrepancies, however, are minor and ultimately negligible. For purely volcanoclastic and plutonic muds, α_E^{Al} values were calculated with reference to the average composition of their magmatic source rocks (median of the available published analyses) rather than to UCC (standards used for normalization and calculation of weathering indices are provided in the auxiliary material).¹

[22] Several other geochemical parameters may reflect weathering, such as the ratio between different non-mobile elements (e.g., Al/Ti, Ga/Al) [Shiller and Frilot, 1996; Young and Nesbitt, 1998] or REE behavior [McLennan, 1989]. A more negative Eu anomaly may be caused by the selective removal of Eu-rich feldspar, a positive Ce anomaly may form in lateritic profiles beneath horizons of Fe oxide accumulation [Braun *et al.*, 1990; Brown *et al.*, 2003], and prominent MREE bulges [Haley *et al.*, 2004] are potentially caused by selective weathering of MREE-rich apatite relative to LREE-rich monazite or HREE-rich xenotime and zircon [Middleburg *et al.*, 1988].

3.3. Sr and Nd Isotopic Ratios

[23] Quartered aliquots of the pristine fractions of 38 samples were sieved at 63 μm to eliminate sand. Subsequently, they were leached in concentrated HCl [Nägler and Kamber, 1996], then digested using a HNO_3 -HF mixture for 24 h at approximately 130°C, converted to chloride, spiked, and merged with the first HCl leach. Column chemistry for Rb, Sr, Sm, and Nd is after Büttner *et al.* [2005]. Sr measurements by multicollector ICP-MS required additional purification by using the Sr-Spec[®] resin. All analyses were performed on Nu-Instruments[®] at the University of Bern. Intralaboratory repeatability was monitored by analyses of NIST SRM 987 and of La Jolla Nd standard. During the measuring sessions, the standard deviation for seven replicate

analyses was 0.710161 ± 7 for $^{87}\text{Sr}/^{86}\text{Sr}$ ratios and 0.511829 ± 6 for $^{143}\text{Nd}/^{144}\text{Nd}$ ratios. Measured isotopic ratios are normalized to $^{86}\text{Sr}/^{84}\text{Sr}=0.1194$. $^{143}\text{Nd}/^{144}\text{Nd}$ ratios are relative to $^{146}\text{Nd}/^{144}\text{Nd}=0.7219$ [Lugmair *et al.*, 1975]. The $^{143}\text{Nd}/^{144}\text{Nd}$ ratio is expressed as present-day $\epsilon\text{Nd}_{(0)}$ using the present-day chondritic uniform reservoir value 0.512638 [Wasserburg *et al.*, 1981]. From the $^{143}\text{Nd}/^{144}\text{Nd}$ and $^{147}\text{Sm}/^{144}\text{Nd}$ ratios of analyzed mud samples, model mantle derivation ages (t_{DM}) were calculated according to Nägler and Kramers [1998], with uncertainties conservatively taken as 0.1 Ga.

4. Mud Mineralogy and Geochemistry in the East African Rift

[24] Along divergent plate margins, sediments are derived from volcanic, plutonic, metamorphic, and sedimentary rocks in various proportions, depending primarily on areal distribution of magmatic activity, rift-shoulder tectono-stratigraphy, and intensity and duration of tectonic uplift associated with rifting. Recycling of syn-rift sediments also occurs. Such distinct mineralogical signatures, fully displayed by modern sediments along the Red Sea and Gulf of Aden rifts in arid tropical areas to the north (“Volcanic Rift” and “Rift Shoulder” Provinces) [Garzanti *et al.*, 2001; Garzanti and Andò, 2007], are progressively blurred by chemical weathering toward the wetter equatorial latitudes of the East African Rift. Whereas sand petrography provides more complete and easily readable information on parent rocks, integrated information on mineralogy and chemistry of muds reveals much of their weathering history.

[25] The intensity of chemical weathering depends on several interplaying factors, including climatic conditions as well as the amount of available time [Drever, 1994; White and Blum, 1995; Taylor and Howard, 1999]. Compositional signatures inherited from source rocks tend to be preserved where topographic relief is steep and erosion rapid enough (weathering-limited conditions). But wherever weathering rates exceed the ability of transport processes to remove material (transport-limited conditions), rocks and soils exposed for longer periods of time are progressively leached, until the sedimentary product becomes strongly depleted in soluble cations [Stallard, 1988; Johnsson, 1993].

[26] River muds were grouped in homogenous sedimentary “provinces” (i.e., geographic areas characterized by similar bedrock lithology and

¹All Supporting Information may be found in the online version of this article.

geomorphology, resulting in analogous petrographic, mineralogical, and chemical composition), which are displayed in Figure 2 and represent the basis for the following descriptions. We will illustrate first the mineralogical and geochemical signatures of volcanoclastic, metamorphiclastic, plutoniclastic, and sedimentoclastic or meta-sedimentoclastic muds produced in regions with contrasting weathering intensities, and next the compositional evolution associated with mixing of sediments carried by diverse tributaries downstream the Kagera-Nile from Burundi and Rwanda highlands to South Sudan.

[27] The main mineralogical and geochemical parameters illustrating mud composition in different sedimentary provinces are summarized in Table 1, whereas Rb-Sr and Sm-Nd isotopic data are presented in Table 2. The complete mineralogical and geochemical database is provided in the auxiliary material, which also contains a synthetic description of each identified sedimentary province and the detailed account of mineralogical, geochemical, and isotope signatures characterizing each. Relative contributions from volcanic rocks to Rusizi and Nyabarongo muds were quantified mathematically by forward end-member modeling of geochemical data [Garzanti *et al.*, 2012].

4.1. Mud From Neogene Basalts

[28] Mud of “Volcanic Rift Provenance” derived from relatively arid areas in the rain shadow of the Virunga volcanoes is dominated by only slightly weathered bedrock minerals (plagioclase, sanidine, pyroxene), Fe oxides, and amorphous matter (volcanic glass). Secondary clay minerals are negligible even in rill sediment, indicating only minor weathering and very immature soils. Chemical composition reflects limited weathering of basaltic source rocks. Muds are moderately depleted in alkali and alkaline-earth metals relative to sand and parent lavas [Rogers *et al.*, 1992; 1998]. In the wetter and lower altitude South Kivu Province, mud is dominated by amorphous matter (including altered glass), clay minerals, and Fe oxides/hydroxides. Kaolinite dominates over smectite and illite (Figure 4). Concentrations of Mg, Ca, Na, and Sr are an order of magnitude lower than in parent lavas [Furman and Graham, 1999], indicating extreme weathering. South Kivu mud is poorer in all alkali and alkaline-earth metals relative to Virunga muds.

4.2. Mud From Paleoproterozoic Basements

[29] Muds of “Dissected Rift-Shoulder Provenance” produced along the western, drier inner flank of the

Kivu-Tanganyika rift shoulder include micas, clay minerals, quartz, and significant feldspars. Kaolinite prevails over illite and locally smectite in tributaries of Lake Kivu, or minor chlorite in tributaries of Lake Tanganyika. The drier intervening Rusizi basin is characterized by illite-kaolinite-smectite assemblages with minor chlorite (Figure 4). Although displaying higher concentrations than in sands, alkali and alkaline-earth metals are depleted by over an order of magnitude relative to UCC in all mud samples. Ca, Na, and Sr are significantly depleted also relative to PAAS, suggesting breakdown of plagioclase. Upper Rusizi mud at the southern edge of the South Kivu lava field shows consistently higher concentrations of Fe, Ti, P, Mn, V, Nb, Ta, Co, Ni, Cu, and Zn than in basement-derived mud, indicating a volcanic contribution $\leq 13\%$. Slightly higher concentrations of Fe, P, Mn, V, Co, Ni, and Cu are maintained down to the delta in Lake Tanganyika, indicating an overall volcanic contribution $\leq 6\%$. Such a low volcanic contribution to the total sediment, considering that Neogene volcanic rocks occupy much of the upper catchment and $\sim 22\%$ of the entire Rusizi catchment [Soreghan and Cohen, 1993], is consistently indicated also by forward-mixing calculations based on mineralogical and geochemical data on sand. In spite of active block faulting and localized slope instability [Ilunga, 1991; Moeyersons *et al.*, 2004], erosion rates and sediment production are thus inferred to be rather low in most of the South Kivu volcanic field, due to a combination of limited intermittent uplift and extensive vegetation cover.

[30] Along the eastern, wetter outer flank of the Kivu-Tanganyika rift shoulder, muds include less feldspars (mainly K-feldspar) and more clay minerals. Kaolinite dominates over illite and chlorite, and it is the virtually exclusive clay mineral in the Nyungwe Forest rill sample. Smectite is absent. Alkali and alkaline-earth metals are most strongly depleted in the Nyungwe and Muramvya Provinces and display similar concentration as in sands. Decreasing weathering toward less humid northern Rwanda is indicated by less pronounced depletion in the Gishwati Province; Al, K, and Rb are relatively abundant, suggesting selective preservation of muscovite. Eu anomalies are commonly markedly negative, reflecting felsic protoliths and extensive feldspar dissolution. However, Eu anomalies less negative than UCC and high concentrations in Fe, Mn, Sc, Co, and other metals may reflect metabasite protoliths in the Muramvya Province as far north as the Rwanda-Burundi border, as indicated by common epidote and amphibole in sands [Garzanti *et al.*, in review].

Table 1. Mineralogy and Chemistry of Mud in the East African Rift^a

Provinces	N	Qz	Kf	Pl	tHM	FeOx	Mica	Clay	amorph.	Kln	Sme	Ill	Chl	CIA	WIP	$\alpha^{\text{Al}}\text{Na}$	$\alpha^{\text{Al}}\text{Ca}$	$\alpha^{\text{Al}}\text{Sr}$	$\alpha^{\text{Al}}\text{Mg}$	$\alpha^{\text{Al}}\text{K}$	$\alpha^{\text{Al}}\text{Ba}$	La _N /Sm _N	Gd _N /Ho _N	Ho _N /Y _N	Eu/Eu*	
Volcaniclastic Muds																										
Virunga	5	1	14	17	17	11	6	0	35	100.0	—	—	—	60	62	1	2	2	6	1	2	5.7	2.7	1.1	0.69	
Virunga rill	1	1	20	35	25	15	5	0	0	100.0	—	—	—	51	33	3	1	1	3	2	1	4.7	2.3	1.1	0.79	
South Kivu	1	7	1	0	0	15	2	25	50	100.0	79	13	8	0	100.0	99	5	38	15	16	3	4.0	2.0	1.2	0.87	
Plutoniclastic Muds																										
Victoria Nile	1	21	19	10	0	10	12	7	21	100.0	57	4	39	0	100.0	68	47	4	2	5	1	3.5	2.6	1.4	0.40	
Gitarama	2	36	16	2	0	2	7	21	17	100.0	53	15	32	0	100.0	82	24	13	2	4	1	3.8	1.8	1.1	0.43	
Metamorphiclastic Muds																										
Kivu	2	18	7	6	0	1	42	28	0	100.0	58	9	34	0	100.0	85	30	9	7	4	2	4.0	2.1	1.0	0.55	
Rusizi	5	17	4	5	1	1	41	28	4	100.0	35	24	40	2	100.0	78	33	6	10	7	2	3.6	1.4	0.9	0.62	
Tanganyika	3	21	9	7	5	3	23	21	12	100.0	58	0	39	4	100.0	80	33	7	6	8	2	3.8	1.6	1.0	0.42	
Gishwati	2	12	4	2	0	2	39	43	0	100.0	67	0	33	0	100.0	83	37	16	20	9	5	3.9	2.4	1.1	0.53	
Nyungwe	8	16	3	1	0	5	35	41	0	100.0	78	0	22	0	100.0	90	18	13	5	2	2	3.9	1.9	1.0	0.44	
Nyungwe rill	1	23	2	2	0	8	27	39	0	100.0	94	0	6	100.0	91	15	18	17	5	3	5	3.2	1.4	0.8	0.43	
Muramvya	5	23	6	4	1	4	19	28	16	100.0	86	0	15	0	100.0	92	11	56	16	6	4	4.0	1.4	0.9	0.67	
Meta-sedimentalastic Muds																										
W. Domain (Rwanda)	9	26	4	2	1	7	28	20	13	100.0	47	0	53	0	100.0	85	14	19	15	5	2	4.3	1.5	1.0	0.64	
W. Domain (Burundi)	6	27	3	0	0	4	8	15	43	100.0	74	0	27	0	100.0	92	11	30	15	7	9	4.4	1.4	1.0	0.59	
W. Domain rill	1	28	1	1	0	0	18	27	25	100.0	65	0	35	0	100.0	93	9	39	95	9	14	4.3	1.4	1.0	0.68	
Sedimentalastic Muds																										
Eastern Domain	2	38	3	3	0	3	5	14	33	100.0	28	31	41	0	100.0	82	20	21	10	6	2	4.2	1.5	1.0	0.67	
Malagarasi	5	17	4	5	0	1	37	37	0	100.0	71	0	29	0	100.0	83	31	10	21	8	4	4.0	1.7	0.9	0.57	
Kagera Basin	3	8	2	1	0	7	35	49	0	100.0	81	0	19	0	100.0	91	18	28	24	10	7	4.2	1.8	1.0	0.67	
Nyabarongo	2	38	2	0	0	3	11	12	36	100.0	79	0	21	0	100.0	91	10	16	12	5	3	3.3	1.3	0.9	0.44	
Ruvyironza	3	21	3	1	0	4	18	26	30	100.0	81	0	19	0	100.0	91	13	26	19	10	7	4.0	1.5	1.0	0.59	
Ruvubu	5	19	3	2	0	3	19	23	32	100.0	61	5	35	0	100.0	86	15	14	12	5	6	4.4	1.4	1.0	0.61	
Kagera	2	54	11	1	0	0	9	10	15	100.0	71	9	20	0	100.0	93	7	59	28	8	11	6.2	1.4	0.9	0.55	
White Nile Basin	2	54	11	1	0	0	9	10	15	100.0	71	9	20	0	100.0	93	7	59	28	8	11	6.2	1.4	0.9	0.55	
S Uganda	2	54	11	1	0	0	9	10	15	100.0	71	9	20	0	100.0	93	7	59	28	8	11	6.2	1.4	0.9	0.55	
Lake Albert	2	54	11	1	0	0	9	10	15	100.0	71	9	20	0	100.0	93	7	59	28	8	11	6.2	1.4	0.9	0.55	
Albert Nile	1	54	11	1	0	0	9	10	15	100.0	71	9	20	0	100.0	93	7	59	28	8	11	6.2	1.4	0.9	0.55	

^aN = number of samples; Q = quartz; Kf = K-feldspar; Pl = plagioclase; tHM = transparent heavy minerals (chiefly pyroxene or amphibole); FeOx = iron oxides (chiefly magnetite or hematite); amor. = amorphous material (volcanic glass, organic matter); Kln = kaolinite; Sme = smectite; Ill = illite; Chl = chlorite; CIA = Chemical Index of Alteration; WIP = Weathering Index; α^{Al} values were normalized to non-mobile Al and calculated with reference to average Virunga [Rogers et al., 1992, 1998] and Kivu lavas [Furman and Graham, 1999] for purely volcaniclastic muds, to Kibaran and Singo granitoids [Fernandez-Alonso et al., 1986; Fernandez-Alonso and Theunissen, 1998; Nagudi et al., 2003] for purely plutoniclastic muds, and to UCC for all other mud samples. The Eu anomaly Eu/Eu* and the chondrite-normalized La_N/Sm_N, Gd_N/Ho_N, and Ho_N/Y_N ratios are also given.

4.3. Mud From Precambrian Granitoids

[31] Feldspars are abundant and K-feldspar prevalent over plagioclase in muds derived from both Gitarama and Mutara Granites in central and NE Rwanda, but the plagioclase/feldspar ratio is higher in the former. Clay minerals include kaolinite, illite, and smectite in both provinces. Alkali and alkaline-earth metals are only slightly depleted in Victoria Nile sediments at Itanda falls. Instead, depletion particularly in Na, Ca, and Sr is significant in Gitarama mud and strong in Mutara mud compared to parent Kibaran granitoid rocks [Hildebrand, 1984; Fernandez-Alonso *et al.*, 1986; Fernandez-Alonso and Theunissen, 1998]. REE patterns locally display more negative Eu anomaly than in granitoid bedrock, reflecting feldspar dissolution.

4.4. Mud From Mesoproterozoic Cover Strata

[32] Muds of “Transitional Rift-Shoulder Provenance” derived from Western Domain meta-sediments include quartz, Fe oxides/hydroxides, and few feldspars (K-feldspar > plagioclase). Illite and kaolinite are equally abundant in Rwanda, whereas kaolinite prevails in Burundi (Figure 4). Gibbsite was recorded locally. Smectite is absent. Strong depletion of mobile alkali and alkaline-earth metals reflects both intense weathering and dilution by quartz derived from metapsammite protoliths, as reflected by low WIP particularly in sand. The rill sample is strongly depleted in Mg and Ca but otherwise similar to fluvial mud. Eu anomalies are as low as 0.36. Similar mineralogy and geochemistry characterize muds of “Undissected Rift-Shoulder Provenance” derived from siliciclastic units of the Eastern Domain, where the CIA may reach up to 93 due to extreme depletion in Na and Ca.

4.5. Malagarasi Basin

[33] Muds derived from Proterozoic siliciclastic and volcanic cover rocks with minor contributions from the Tanzania Craton are invariably dominated by quartz, with minor feldspars (mostly K-feldspar). Smectite, illite, and kaolinite are all common (Figure 4). Low concentrations in alkali and alkaline-earth metals are largely ascribed to dilution by recycled quartz, whereas relatively high concentrations in Fe, Mg, Mn, V, Co, Ni, Cu, and Eu anomaly slightly less negative than UCC reveal contribution from Neoproterozoic basalts.

4.6. Kagera Basin

[34] Muds in the upper catchment include micas and clay minerals (predominant in Nyabarongo and Akanyaru muds), quartz (most abundant in Ruvubu muds), and subordinate feldspars. K-feldspar and plagioclase are equally abundant in Nyabarongo muds. Although Ruvubu muds are generally feldspar-poor, K-feldspar is common in the headwaters, reflecting provenance from syenites of the Upper Ruvubu alkaline complex. Kaolinite invariably dominates over illite. Mineralogy is intermediate between Nyabarongo and Ruvubu muds downstream of their confluence, indicating sub-equal mud supply from these two rivers. Kaolinite decreases and smectite becomes significant along the lower Kagera, suggesting that up to 50% of the mud carried to Lake Victoria may be produced in the lower catchment.

[35] Mud geochemistry fails to indicate any effect of progressive maturation in alluvial storage sites. On the contrary, CIA and α^{Al} values are highest in Nyabarongo headwaters (Nyungwe Province) and decrease downstream, where they become similar to those of muds in the Gishwati Province characterized by less humid climate and higher rates of physical erosion. Alkali and alkaline-earth metals (particularly Sr), Ti, Nb, and Ta are higher in Mukungwa mud than in the Gishwati Province, and the same elements increase in Nyabarongo mud downstream of the Mukungwa confluence, indicating significant mud supply from the Virunga volcanoes ($\leq 30\%$ to Mukungwa mud; $\leq 10\%$ to Nyabarongo mud). Such estimated volcanic contributions are considerably higher than those estimated with forward-mixing calculations based on mineralogical and geochemical data on sand [Garzanti *et al.*, in review]. Supply from the Akanyaru River is probably subordinate because all chemical parameters are virtually unchanged downstream of the Akanyaru confluence.

[36] Ruvyironza and Ruvubu muds are strongly depleted in mobile elements because of both intense weathering and quartz dilution. In their lower course, muds become enriched in Cr and Ni, revealing a contribution from Kibaran mafic-ultramafic-layered intrusions. Lower Kagera muds are enriched in Si due to further quartz dilution.

4.7. Uganda and the Nile

[37] Mud carried by the Ruizi River is quartzose with minor K-feldspar. Kaolinite dominates over illite and smectite. High concentration of Si, Zr, and Hf, as well as very low alkali and alkaline-earth

Table 2. Sr and Nd Isotopic Data. GSZ = Analyzed Grain-Size Fraction (in Microns)

Sample	River	Site	Deposit	GSZ	Rb (ppm)	Sr (ppm)	Rb/Sr	⁸⁷ Rb/ ⁸⁶ Sr	⁸⁷ Sr/ ⁸⁶ Sr	2 σ	Sm (ppm)	Nd (ppm)	Sm/Nd	¹⁴⁷ Sm/ ¹⁴⁴ Nd	2 σ	¹⁴³ Nd/ ¹⁴⁴ Nd	2 σ	ε _{Nd0}	f _{DM} (Ga)	
Virunga and S Kivu Volcanic Provinces																				
S 3896	Muhe	Ruhengeri	Mud	<63	30	213	0.14	0.4016	0.0002	0.71107	0.00003	7	44	0.16	0.0949	0.0003	0.512097	0.000003	-11	1.35
S 3895	Susa	Ruhengeri	Mud	<63	40	119	0.34	0.9704	0.0007	0.70744	0.00002	8	52	0.15	0.0928	0.0003	0.512300	0.000003	-7	1.07
S 3866	Shangazi	Bushenge	Mud	<63	5	32	0.16	0.4648	0.0196	0.71272	0.00058	8	38	0.21	0.1244	0.0004	0.512660	0.000004	0	0.84
Congo System																				
S 3863	Ruhwa	Rukana	Mud	<63	67	40	1.67	4.8729	0.0737	0.77301	0.00002	4	23	0.19	0.1160	0.0003	0.511541	0.000004	-21	2.49
S 3859	Kaburantwa	Kaburantwa	Mud	<63	40	10	3.85	11.2178	0.0033	0.78632	0.00003	4	19	0.20	0.1186	0.0004	0.511725	0.000005	-18	2.27
S 3856	Rusizi	Gatumba	Mud	<63	60	32	1.88	5.4757	0.0019	0.76970	0.00004	6	29	0.19	0.1172	0.0004	0.511716	0.000003	-18	2.25
S 3839	Rugera	Muyange	Sand	<63	40	84	0.48	1.3772	0.0019	0.72452	0.00003	8	45	0.17	0.1005	0.0003	0.511029	0.000003	-31	2.83
S 3826	Rumpungwe	Gisuru	Sand	<63	68	21	3.25	9.5524	0.2485	0.85992	0.00003	2	9	0.19	0.1175	0.0004	0.511564	0.000007	-21	2.49
S 3831	Ruchugi	Uvinza	Mud	<63	54	22	2.47	7.2234	0.4656	0.80781	0.00004	4	17	0.23	0.1376	0.0004	0.511551	0.000008	-21	3.17
S 3837	Malagarasi	Ilagala	Sand	<63	33	41	0.81	2.3594	0.0004	0.75731	0.00004	4	19	0.22	0.1307	0.0004	0.511772	0.000006	-17	2.51
Kagera system																				
S 3882	Rukarara	Gakangara	Mud	<63	37	9	4.37	12.7221	0.0069	0.78313	0.00004	3	16	0.19	0.1141	0.0003	0.511527	0.000003	-22	2.47
S 3893	Gicye	Gicye	Mud	<63	114	25	4.66	13.6130	0.0236	0.80729	0.00002	7	31	0.21	0.1286	0.0004	0.511824	0.000003	-16	2.36
S 3874	Nyabarongo	Kaduha	Mud	<63	74	22	3.36	9.8266	0.0052	0.81173	0.00002	3	16	0.20	0.1218	0.0004	0.511611	0.000006	-20	2.53
S 3916	Nyabarongo	Kigali	Mud	<63	105	44	2.39	7.0047	0.0025	0.82339	0.00002	6	30	0.19	0.1170	0.0004	0.511678	0.000003	-19	2.31
S 3790	Akanyaru	Kanyaru Haut	Mud	<63	56	18	3.13	9.1325	0.0024	0.80649	0.00003	4	18	0.21	0.1276	0.0004	0.511788	0.000005	-17	2.39
S 3918	Akanyaru	Rutabo	Mud	<63	42	20	2.09	6.0904	0.0901	0.76798	0.00006	3	14	0.20	0.1197	0.0004	0.511823	0.000004	-16	2.14
S 3811	Ruvyironza	Mugera	Mud	<63	31	17	1.81	5.2768	0.0255	0.79222	0.00004	4	20	0.22	0.1313	0.0004	0.511636	0.000004	-20	2.78
S 3792	Ruvubu	Gatara	Mud	<63	38	40	0.96	2.7778	0.0155	0.74263	0.00007	3	17	0.20	0.1185	0.0004	0.511906	0.000006	-14	1.98
S 3792	Ruvubu	Gatara	Mud	Replicate																
S 3792	Ruvubu	Gatara	Mud	Replicate																
S 3823	Ruvubu	Mvano	Mud	<63	53	29	1.82	5.2832	0.0038	0.76525	0.00003	5	25	0.18	0.1105	0.0003	0.512000	0.000004	-12	1.69
S 3921	Muvumba	Kagitumba	Mud	<63	57	47	1.20	3.4954	0.0025	0.75951	0.00004	5	26	0.21	0.1260	0.0004	0.511809	0.000008	-16	2.31
S 3922	Kagera	Kagitumba	Mud	<63	55	41	1.34	3.8977	0.0810	0.76252	0.00002	3	14	0.19	0.1166	0.0003	0.511737	0.000006	-18	2.20
S 3924	Kagera	Kikagati	Mud	<63	98	53	1.87	5.4310	0.1019	0.75499	0.00003	3	16	0.20	0.1211	0.0004	0.511784	0.000005	-17	2.23
S 3643	Kagera	Kyaka	Sand	<63	35	47	0.75	2.1889	0.0337	0.74791	0.00005	6	31	0.19	0.1172	0.0004	0.512083	0.000003	-11	1.68
S 3643	Kagera	Kyaka	Sand	Replicate																
S 3641	Kagera	Kasensero	Sand	<63	69	66	1.04	3.0207	0.0014	0.74961	0.00003	12	65	0.18	0.1083	0.0003	0.511943	0.000005	-14	1.74
S 3641	Kagera	Kasensero	Sand	<63	37	44	0.84	2.4469	0.0438	0.74712	0.00004	6	31	0.20	0.1189	0.0004	0.511747	0.000009	-17	2.24
White Nile System																				
S 3777	Ruizi	Mbarara	Mud	<63	18	17	1.06	3.0951	0.0521	0.76736	0.00003	8	46	0.18	0.1072	0.0003	0.511382	0.000002	-24	2.51
S 3701	Sezibwa	Sezibwa Falls	Sand	<63	22	68	0.33	0.9530	0.0022	0.72729	0.00003	4	20	0.20	0.1235	0.0004	0.511731	0.000004	-18	2.38
S 3701	Sezibwa	Sezibwa Falls	Sand	Replicate																
S 3698	Kafu	Kibangya	Sand	<63	42	77	0.55	1.5964	0.0021	0.76600	0.00017	8	43	0.20	0.1216	0.0004	0.511755	0.000007	-17	2.29
S 3676	Mubuku	Mubuku	Sand	<63 silt	40	80	0.50	1.4560	0.0004	0.73251	0.00003	3	18	0.18	0.1097	0.0003	0.511393	0.000004	-24	2.56
S 3676	Mubuku	Mubuku	Sand	clay	44	52	0.85	2.4714	0.0017	0.73722	0.00006	4	22	0.17	0.1036	0.0003	0.511424	0.000004	-24	2.37
S 3677	Rwimi	Rwimi	Sand	<63	28	136	0.20	0.5913	0.0018	0.72304	0.00002	7	45	0.15	0.0923	0.0003	0.512001	0.000004	-12	1.44
S 3677	Rwimi	Rwimi	Sand	Replicate																
S 3680	Nkusi	Pachwa	Sand	<63	58	38	1.52	4.4414	0.0821	0.79975	0.00004	9	48	0.18	0.1076	0.0003	0.512044	0.000004	-12	1.43
S 3696	Waiga	Rabongo Forest	Sand	<63 silt	39	121	0.32	0.9204	0.0053	0.71749	0.00003	6	35	0.19	0.1126	0.0003	0.512090	0.000004	-33	3.13
S 3696	Waiga	Rabongo Forest	Sand	clay	36	45	0.80	2.3275	0.0003	0.72806	0.00008	4	23	0.18	0.1109	0.0003	0.511359	0.000003	-25	2.63
S 3700	Victoria Nile	Itanda Falls	Sand	<63	86	541	0.16	0.4595	0.0003	0.71536	0.00003	22	139	0.16	0.0954	0.0003	0.510782	0.000007	-36	3.02
S 3692	Victoria Nile	Murchison Falls	Sand	<63	34	281	0.12	0.3454	0.0058	0.71357	0.00004	8	41	0.21	0.1248	0.0004	0.511122	0.000005	-30	3.44
S 3689	Ora	Wadelai	Sand	<63	53	377	0.14	0.4092	0.0006	0.72157	0.00004	5	26	0.18	0.1102	0.0003	0.510983	0.000011	-32	3.16
S 3690	Albert Nile	Wadelai	Sand	<63	66	250	0.27	0.7705	0.0033	0.71954	0.00004	11	64	0.18	0.1087	0.0003	0.510934	0.000007	-33	3.19
S 4052	Bahr el Jebel	Juba	Sand	<63	83	302	0.27	0.7910	0.0005	0.71552	0.00004	6	30	0.18	0.1103	0.0003	0.511346	0.000016	-25	2.64

metals, suggests recycling of quartz and zircon from meta-sedimentary sources. Extreme weathering, instead, is indicated for Si-poor Katonga mud produced in Uganda lowlands. Depletion in most elements in Si-rich muds of the northern Lake Albert graben and Albert Nile outlet indicates local recycling from quartzose Neogene rift sediments (“Recycled Clastic Provenance”), rather than extensive weathering. In Albert Nile mud downstream, higher ratios of most chemical elements to Si reflect dominant first-cycle contribution from high-grade basement rocks of northern Uganda.

5. Isotope Signatures

[38] The analysis of Rb-Sr and Sm-Nd isotopic systems in river sediments gives a weighted average of rock units eroded in the drainage basin and has been used to obtain information on crustal evolution and composition as well as on weathering processes [Goldstein *et al.*, 1984; Allègre *et al.*, 1996]. Isotope geochemistry also helps us to assess relative sediment contributions from diverse sub-catchments and thus to calculate sediment fluxes and infer regional erosion patterns. Rivers draining older crust have relatively more radiogenic Sr and non-radiogenic Nd than those draining younger crust, and there is thus a broad inverse relationship between $^{87}\text{Sr}/^{86}\text{Sr}$ and $\epsilon\text{Nd}_{(0)}$. REE are non-mobile elements, and the Sm-Nd isotopic system is generally held as insensitive to weathering [Nesbitt and Markovics, 1997; Gaillardet *et al.*, 2003]. Conversely, Sr is highly mobile, and thus both dissolved and suspended load Sr must be considered in determining the average Rb-Sr isotopic systematics of drainage basins. Nevertheless, although the $^{87}\text{Rb}/^{86}\text{Sr}$ ratio is fractionated due to Rb and Sr mobility during weathering, the $^{87}\text{Sr}/^{86}\text{Sr}$ ratio of total river load is generally observed to robustly lie within the range of values displayed by source rocks [Goldstein and Jacobsen, 1988].

[39] In order to check for grain-size control on isotopic signatures, we analyzed the silt and clay fractions separated by sieving and settling from two sand samples (Mubuku and Waiga). In both cases, the clay fraction yielded higher $^{87}\text{Sr}/^{86}\text{Sr}$ (reflecting its higher Rb/Sr ratio), indistinguishable $\epsilon\text{Nd}_{(0)}$ and t_{DM} model ages younger by 0.2 Ga (reflecting its lower Sm/Nd ratio) (Table 2).

5.1. Sr and Nd Isotope Data

[40] Isotopic signatures of Virunga muds are compatible with those of parent lavas and closer to those of basanites for Susa mud and to those of

latites for Muhe mud chiefly derived from the Sabinyo volcano. The significantly higher $^{87}\text{Sr}/^{86}\text{Sr}$ ratio in South Kivu mud than in parent lavas can be accounted for by mixing with minor detritus from Precambrian meta-sedimentary wall rocks [Garzanti *et al.*, in review].

[41] High $^{87}\text{Sr}/^{86}\text{Sr}$ ratios are recorded throughout the Kagera basin and in diverse major rivers from SW Uganda to Tanzania (Figure 5a), reflecting widespread exposure of Precambrian granitoid and meta-sedimentary rocks. $^{87}\text{Sr}/^{86}\text{Sr}$ ratios reach close to 0.8 wherever Rusizian or Buganda-Toro gneissic basements are exposed along the rift shoulder. Within the Karagwe-Ankole Belt, $^{87}\text{Sr}/^{86}\text{Sr}$ ratios are invariably above 0.74, thus never revealing supply from Kibaran mafic-ultramafic complexes, and locally exceed 0.80, reflecting input from tin granites and pegmatites or mica-rich meta-sediments (e.g., Gishwati Province). Mud with $^{87}\text{Sr}/^{86}\text{Sr}$ ratios of ~ 0.8 have in fact Rb/Sr ratios an order of magnitude higher than UCC (3.5 ± 1.5 vs. 0.3), reflecting either abundance of mica or very low plagioclase content. In muds from the Karagwe-Ankole Belt, $\epsilon\text{Nd}_{(0)}$ is mostly between -20 and -16 , a range only slightly higher than that of Kibaran intrusions. $\epsilon\text{Nd}_{(0)}$ tends to become more strongly negative northward across Uganda, reflecting widespread exposure of older Paleoproterozoic to Archean terranes (Figure 5a).

[42] Victoria and Albert Nile muds display the lowest $^{87}\text{Sr}/^{86}\text{Sr}$ ratios and most negative $\epsilon\text{Nd}_{(0)}$ of our entire sample set, and similar or slightly higher values characterize muds carried by their tributaries Ora and Waiga. Most strongly negative $\epsilon\text{Nd}_{(0)}$ in these samples is explained by the Archean age of basement rocks in Uganda, whereas their lower $^{87}\text{Sr}/^{86}\text{Sr}$ ratio relative to basement-derived muds in Burundi and Rwanda reflects an order of magnitude lower Rb/Sr ratios (0.2 ± 0.1), resulting in turn from lower mica/plagioclase ratios in higher-grade mid-crustal parent rocks. The same holds true for mud derived from the Tanzania Craton in SW Burundi.

[43] $^{87}\text{Sr}/^{86}\text{Sr}$ ratios are a good tracer of sediment provenance in the Kagera basin, where different trends are displayed along its diverse tributaries. The value shown by lower Ruvubu mud, intermediate between the high value of Ruvyironza mud and the relatively low value of upper Ruvubu mud, indicates similar supply from these two river branches. $^{87}\text{Sr}/^{86}\text{Sr}$ ratios increase progressively downstream the Nyabarongo, indicating major contribution from tributaries of the Gishwati Province and minor supply from the Virunga volcanoes.

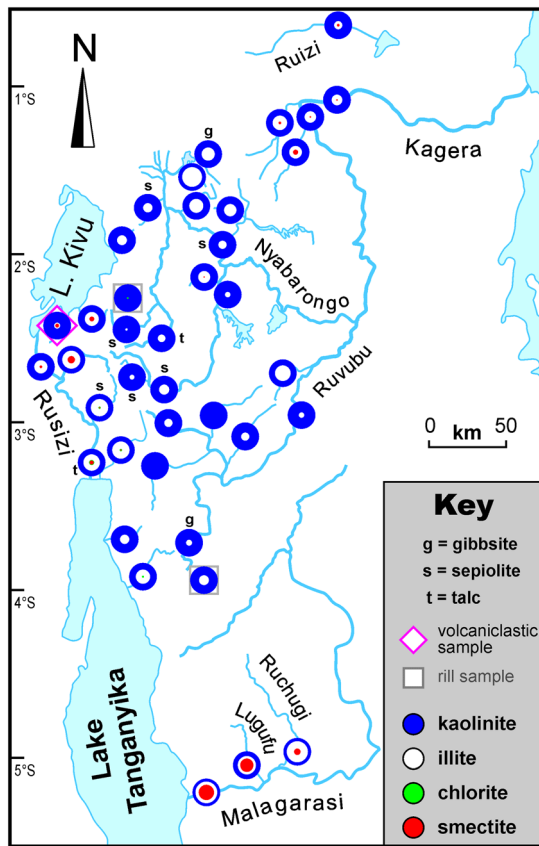


Figure 4. Geographic distribution of clay minerals (circle diameters are proportional to relative mineral abundances). Kaolinite, the typical product of equatorial weathering, is dominant through most of the study area. Smectite characterizes volcaniclastic as well as plutonic and metamorphic mud, from the South Kivu region and Rusizi basin to the lower Kagera, Ruizi, and Malagarasi Rivers draining savannah lowlands of Rwanda, Uganda, and Tanzania. Illite may be locally dominant in muds derived from Mesoproterozoic meta-sediments in Burundi and Rwanda, where gibbsite was occasionally detected. Minor chlorite frequently occurs in muds of Burundi rivers draining toward Lake Tanganyika.

Instead, $^{87}\text{Sr}/^{86}\text{Sr}$ ratios decrease downstream the Akanyaru, which may suggest that sediments from the upper reaches are largely deposited in swampy lowlands and partly replaced by local sediment supply. Sediment storage in lowland swamps, and consequent partial decoupling of the sediment-routing system from headwater sources, apparently occurs also further downstream along the Kagera, where $^{87}\text{Sr}/^{86}\text{Sr}$ ratios are lower than for all upland branches and close to muds carried by the largest local tributary (Muvumba). In both Kagera and Malagarasi basins, $^{87}\text{Sr}/^{86}\text{Sr}$ ratios tend to decrease downstream towards Lakes Victoria and Tanganyika,

whereas they are homogeneously high through the Rusizi basin, reflecting major contributions from gneissic basement exposed in the Kibira Forest and minor supply from the South Kivu basaltic field.

5.2. Model Ages

[44] Neogene lavas and muds derived from them yield Neoproterozoic to Mesoproterozoic model ages, in contrast with the much younger t_{DM} ages of muds from the Oligocene Ethiopian Traps, characterized by lower $^{87}\text{Sr}/^{86}\text{Sr}$ ratios and positive $\varepsilon\text{Nd}(0)$ [Padoan *et al.*, 2011]. These old ages reflect the long history and complex structure of the underlying lithosphere [Rogers *et al.*, 1998].

[45] Mud derived from metamorphic and plutonic rocks throughout the Kagera and Rusizi basins yield mostly early Paleoproterozoic model ages (Figure 5b). These reflect the isotopic signatures of both Rusizian basement and Kibaran to post-Kibaran felsic and mafic intrusions, which in turn are the product of repeated reworking and re-melting of early Paleoproterozoic crust through the late Paleoproterozoic and Mesoproterozoic [Tack *et al.*, 2010]. Upper Ruvubu mud yields a notably younger model age, reflecting supply from the Neoproterozoic Upper Ruvubu alkaline plutonic suite. An unexpectedly young, Mesoproterozoic t_{DM} model age was obtained for Rwimi mud, derived from the Paleoproterozoic central Rwenzori massif. This would be explained if the sample, which has a higher Nd concentration and a lower Sm/Nd ratio than Mubuku mud derived from the same source, contains even minute amounts of a LREE-rich mineral such as monazite or allanite derived from younger rocks. Archean model ages characterize most muds from NW Tanzania and Uganda, reflecting direct or indirect provenance from the Tanzania and Congo Cratons (Table 2). The earliest Neoproterozoic t_{DM} age of mud derived from the Tanzania Craton in SW Burundi is virtually identical to that of Ruvyironza mud draining Karagwe-Ankole meta-sediments on the opposite side of the Nile-Congo divide, suggesting an ultimate cratonic provenance for Western Domain meta-sediments in this region.

[46] Downstream the Nile, t_{DM} model ages young progressively from Paleoproterozoic, to early Mesoproterozoic, to late Neoproterozoic and finally early Mesoproterozoic, while the river cuts first across the largely Mesoproterozoic Gneissic-Granulitic Complex, next across Neoproterozoic Aruan rocks in northern Uganda [Schlüter, 2008], and eventually across the Saharan Metacraton highly re-mobilized during the Neoproterozoic in South Sudan [Abdelsalam *et al.*, 2002]. The observed

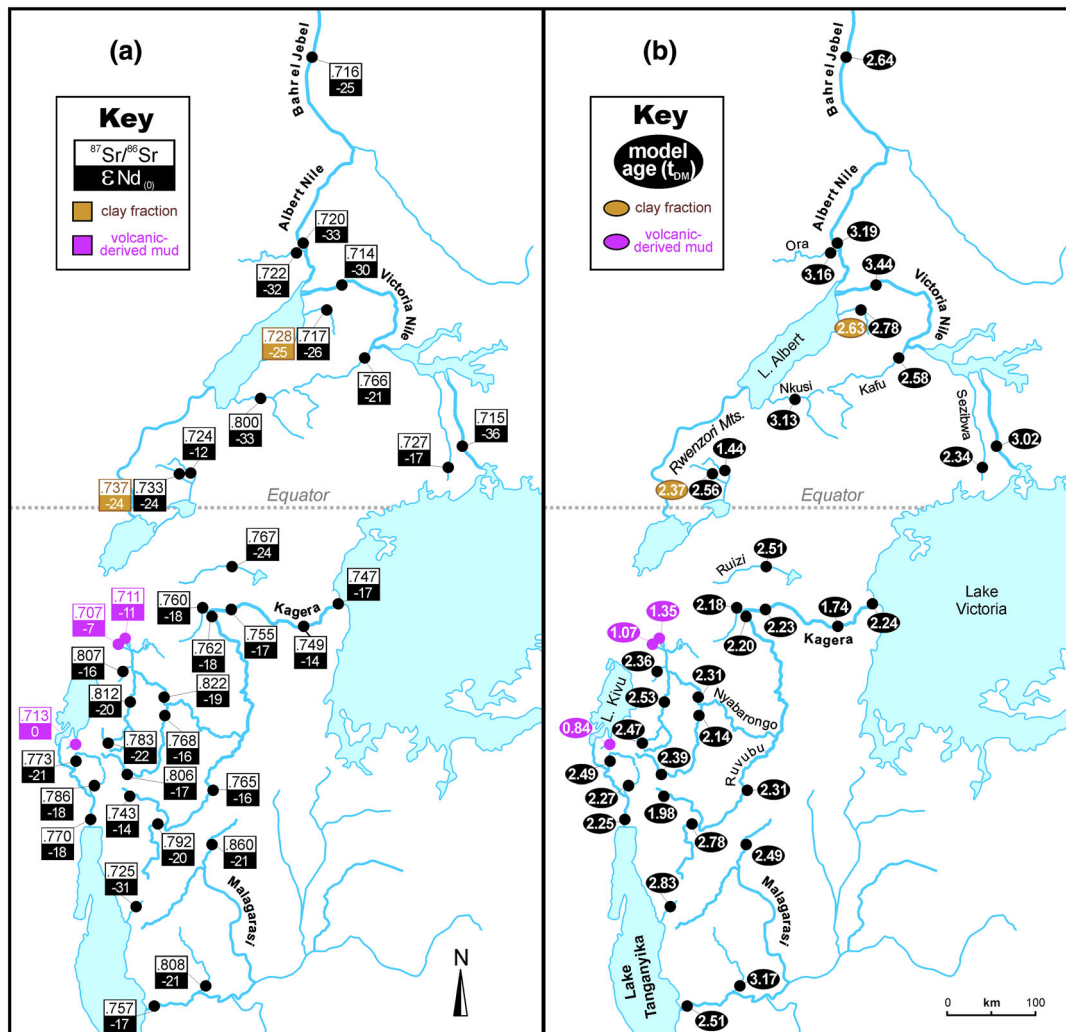


Figure 5. Isotopic signature of muds. (a) $^{87}\text{Sr}/^{86}\text{Sr}$ ratios and $\epsilon\text{Nd}_{(0)}$. Victoria and Albert Nile muds display lower $^{87}\text{Sr}/^{86}\text{Sr}$ and more negative $\epsilon\text{Nd}_{(0)}$ than mud in the Kagera basin, reflecting lack of sediment connection across Lake Victoria. (b) Model mantle derivation ages (t_{DM}). Paleoproterozoic model ages characterize sediments all along the rift shoulders from Burundi to the Rwenzori mountains. Instead, Archean model ages characterize muds of NW Tanzania and Uganda directly or indirectly derived from the Tanzania and Congo Cratons. Much younger Proterozoic ages characterize muds produced in Neogene volcanic fields.

correspondence between model ages of river muds and those of respective parent rocks confirms that the Sm-Nd isotopic system is insensitive to weathering and thus provides a faithful integrated signature of diverse major episodes of crustal growth recorded in the drainage basin.

6. Weathering Control on Sediment Composition

[47] In this section, we will discuss the areal distribution of mineralogical and geochemical parameters, and contrast the behavior of diverse chemical

elements in muds as well as in sands from various parts of the upper Nile and Congo catchments. We will thus investigate where weathering is most intense and why, and by which processes weathering occurs.

6.1. Clay Mineral Distribution

[48] In equatorial soils, high mean annual temperatures foster the aqueous removal of H_4SiO_4 and thereby the formation of clay-mineral assemblages that generally consist of few phases, largely determined by the chemistry of the soil solution. This depends in turn on climatic conditions and especially

on the amount of rainfall and its distribution through the year [Chamley, 1989; Velde, 1995]. The growth of kaolinite usually requires a warm climate with high and evenly distributed rainfall, leading to soil solutions with low concentration of silica and basic cations. Intense leaching prevents the accumulation of organic matter and determines the efficient flushing of mobile elements contained in parent rocks, whereas elements like Al and Ti—with variable amounts of Si and Fe—preferentially remain in the weathering complexes characterized by formation of kaolinite or gibbsite. Abundance of kaolinite requires a permanent groundwater level, whereas a temporary or fluctuating level favors flushing of Si and resulting formation of gibbsite [Wilson, 1999]. Differently from kaolinite, the formation of smectite generally requires a warm climate with rainy seasons separated by a dry season with intense evaporation, leading to soil solutions with high pH and concentrated in silica and basic cations. Such chemical conditions are favored by mafic bedrock, but smectite may be high in soils regardless of parent-rock lithology. During the wet season, especially if temperature is high, hydrolysis is extensive. During the dry season, particularly if longer than the wet one, the ions released from mineral lattices tend to be stored and to concentrate in the soil profile if their normal evacuation is reduced due to only episodic rainfall, presence of an impermeable soil horizon, or naturally high water table. Formation of smectite, typical of tropical vertisols, can thus extend over humid equatorial regions wherever leaching is hampered by low topography and poor drainage conditions.

[49] Along the East African Rift, extensive equatorial weathering results in dominant kaolinite in most analyzed samples. Kaolinite represents >70% of clay minerals in muds produced by alteration of gneissic basement rocks in humid and well-drained rift highlands. Talc or sepiolite, found in laterites formed on mafic or ultramafic substrates [Tauler *et al.*, 2009], occurs locally. Kaolinite reaches 94% in the Nyungwe Forest rill sample lacking both illite and smectite. It represents the only clay mineral in muds of several central Burundi rivers and dominates over smectite and illite even in volcanoclastic mud of South Kivu (Figure 4). Conversely, smectite abounds in drier and poorly drained savannah lowlands and occurs in plutonic muds of NE Rwanda characterized by ustic iso-hyperthermic soils, in muds of NW Tanzania partly derived from Neoproterozoic volcanic rocks, and in muds in SW Rwanda and the Rusizi basin. Even in these regions, however, the kaolinite/smectite ratio is persistently higher than

observed in river muds produced in drier tropical Southern Africa (Figure 6). Illite generally occurs in soils developed under hot wet climate as a residual mineral produced by physical disaggregation of mica-bearing bedrock or feldspar sericitization. It dominates locally in muds derived from low-grade Karagwe-Ankole meta-sediments, occasionally associated with gibbsite. Chlorite is easily weathered in warm humid climate and generally transformed into vermiculite, mixed layers and other clay minerals. It is detected in small quantities in muds from relatively dry westernmost Burundi, as well as in the Nyungwe Forest rill sample collected along the rift-shoulder crest.

6.2. Weathering Geochemistry

[50] Mud in equatorial Africa consistently display a marked depletion in alkali and alkaline-earth metals (Figure 7). Other elements do not show any evident systematic deviation from UCC values, apart from local effects. Hydraulic-sorting or inadvertent contamination by the sand mode during sampling may explain the enrichment in elements preferentially hosted in heavy minerals such as REE and HFSE; quartz dilution explains the depletion of most elements except Si. Ni may be enriched in kaolinite-rich soils [Nyakairu *et al.*, 2001] and lateritic crusts [Maier *et al.*, 2008]. Because of scarcity of carbonate rocks, carbonate weathering plays a negligible role in the East African Rift. Although neither calcite or dolomite were ever detected by mineralogical analyses of muds, intra-basinal calcareous grains may occur in proximity of travertine outcrops or in lacustrine sediments, as hinted at by locally high Ca and Sr in Lake Muhazi and Lake Albert muds.

[51] The comparison of α^{Al} values in various sedimentary provinces (Table 1) allows us to establish an empirical mobility sequence among different mobile elements, controlled by an underlying sequence of mineral stabilities. With a few exceptions, associated with local heterogeneities of parent lithologies, the bulk-sediment mobility sequence consistently observed for mud samples is

$$\alpha_{\text{Na}}^{\text{Al}} > \alpha_{\text{Ca}}^{\text{Al}} > \alpha_{\text{Sr}}^{\text{Al}} > \alpha_{\text{Mg}}^{\text{Al}} > \alpha_{\text{K}}^{\text{Al}} > \alpha_{\text{Ba}}^{\text{Al}} \geq \alpha_{\text{Rb}}^{\text{Al}} > \alpha_{\text{Cs}}^{\text{Al}}$$

indicating that leaching is extreme for Na and Ca, strong for Sr, moderate for Mg and K, minor for Ba and Rb, and minimum for Cs, concordantly with what observed elsewhere [Nyakairu and Koeberl, 2001; Gaillard *et al.*, 2003; Bouchez *et al.*, 2011b]. Small cations (Na, Ca, Sr) are in fact known to be selectively removed from weathering

profiles, whereas larger cations are retained by preferential exchange and adsorption on secondary minerals [Nesbitt *et al.*, 1980]. Rb and Ba are retained relative to K, and Cs (albeit soluble) is so strongly held on clay-mineral surfaces that it can even accumulate in soils [Kronberg *et al.*, 1987; Scarciglia *et al.*, 2011]. Also Be, showing a bulk-sediment mobility close to that of Rb, tends to be retained in, and adsorbed on, clay minerals [Brown *et al.*, 1992].

[52] In humid rift highlands, bulk-sediment mobilities of Na, Ca, Sr, Mg, K, Ba, and Rb appear to be higher—respectively by factors up to 40, 30, 15, 5, 4, 3, and 2—than that of Cs. Such order of bulk-sediment mobility is broadly coherent with the degree into which these elements are partitioned in least stable plagioclase versus K-feldspar and more stable mica, indicating that their behavior is linked to the fate of silicates in which they are preferentially hosted [Nesbitt and Markovics, 1997]. Extreme depletion for Na, Ca, and to a lesser extent Sr in muds derived from gneissic or granitoid rocks (Figure 7) is thus interpreted largely as the consequence of extensive plagioclase weathering in humid rift highlands, whereas in detritus recycled from sedimentary or meta-sedimentary sources, it may simply reflect original scarcity of plagioclase in parent rocks. Assessing the effect of weathering in polycyclic sediments, which are markedly depleted in mobile elements independently of weathering conditions, is a crucial problem that will be dealt with in section 7 below.

6.3. Contrasting Mud and Sand Geochemistry: The Grain-Size Effect

[53] The geochemical differentiation between mud and sand is primarily dependent on the intensity of weathering, subsequently enhanced by hydrologic and hydrodynamic processes [Nesbitt *et al.*, 1996; Bouchez *et al.*, 2011b; Lupker *et al.*, 2011]. In the absence of weathering, mud would contain minor clay minerals and more feldspars, and the compositional contrast with sand would be much weaker. Unsurprisingly, the major differences observed across equatorial Africa include a much greater abundance of quartz in sand (with the exception of volcanoclastic detritus) and of organic matter, clay minerals, and other phyllosilicates in mud. Relative feldspar abundance was observed to be similar in muds and sands of all provinces, and the quartz/feldspar ratio consequently higher in sands, commonly by a factor of 5, which may suggest selective size reduction of more soluble feldspars. Because of such mineralogical diversity, sands are

systematically richer in Si, and muds in most other elements and LOI. Geochemical differences are thus reduced by recalculating compositions to 100% after subtracting SiO₂ and LOI. This rough calculation helped us to enlighten how other elements are partitioned in sand versus mud and thus chiefly in feldspars versus phyllosilicates. Sands are seen to be richer in Na, K, Ca, and Sr (largely hosted in feldspars), whereas Al, Cs, and Ga (largely hosted in phyllosilicates) remain more abundant in muds. Weathering intensity is thus grain-size dependent; the heavier the alkali element, the less depleted in fine-grained relative to coarse-grained sediments [Bouchez *et al.*, 2011b].

[54] Element concentrations in mud samples strongly depend on weathering intensity, because different mineralogical and thus chemical compositions characterize the secondary phases produced by incongruent dissolution of silicates in contrasting climatic and geomorphological conditions. Clay minerals such as kaolinite or Al and Fe oxyhydroxides do not incorporate major cations such as Na, K, Mg, and Ca, which are mainly transported as

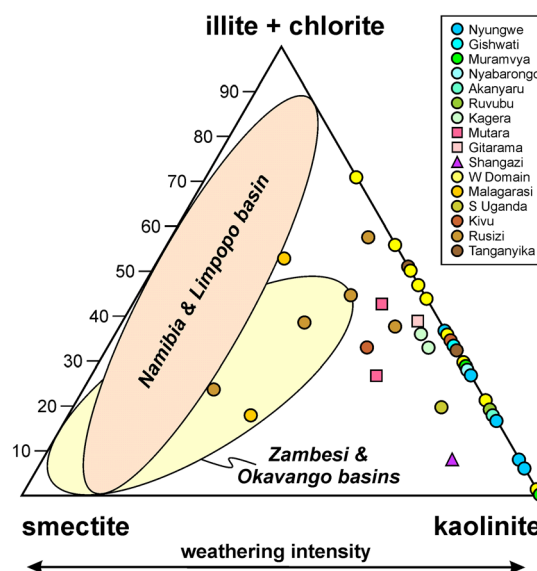


Figure 6. Weathering intensity as revealed by clay-mineral assemblages. Kaolinite is the predominant clay mineral throughout equatorial central Africa, in sharp contrast with drier tropical Southern Africa (Namibia and Limpopo basin) [own data]. Only in the Zambesi and Okavango river systems, sourced in humid sub-equatorial Angola and Zambia, the kaolinite/smectite ratio may approach that of muds produced in drier areas of NW Tanzania and W Burundi (Malagarasi and Rusizi basins).

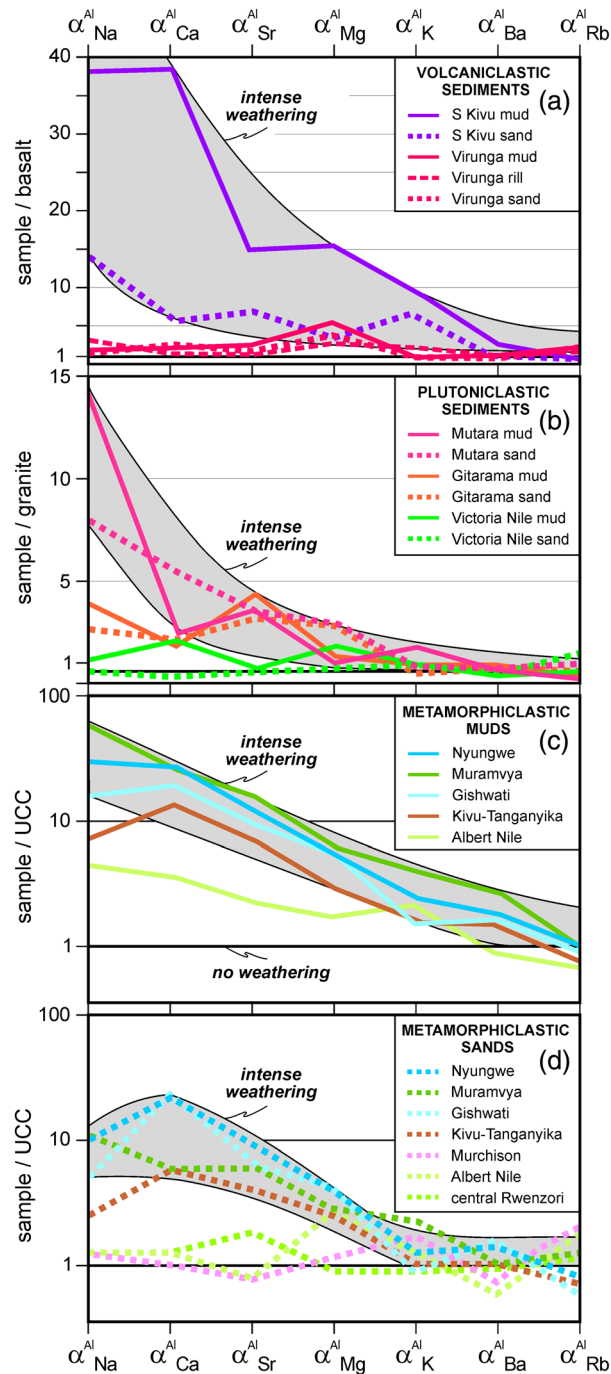


Figure 7. Systematic differential depletion in alkali and alkaline-earth metals. In humid Nyungwe, Muramvya, and Gishwati rift highlands, as well as in the South Kivu and Mutara Provinces, α^{Al} values for Na and Ca typically range from 5 to 20 in sands and from 10 to 50 in muds, whereas for Ba and Rb, they are invariably <5 . In the Virunga Province and Victoria Nile at Itanda Falls, both sands and muds are virtually unweathered ($\alpha^{Al} \sim 1$ for all elements). Gray areas are empirical envelopes for intense equatorial weathering.

dissolved load in rivers [Gaillardet *et al.*, 2003]. Relative to sands, alkali, and alkaline-earth metals are consequently more depleted in kaolinite-rich muds produced in humid rift highlands, than in muds of the lowlands richer in illite and smectite.

[55] Bulk-sediment indices consistently indicate lower weathering for sands than for muds, α^{Al} values being typically half and CIA values lower by 10 to 15 units in sand (Figure 8). Indeed, mud principally derives from mature soil profiles representing the

ultimate product of chemical weathering, whereas coarser detritus chiefly results from physical erosional processes (including landslides involving bedrock, triggered by concentrated rainfall in high-relief areas during the rainy season). The order of bulk-sediment mobility observed for sand samples (Figure 7),

$$\alpha_{\text{Ca}}^{\text{Al}} \approx \alpha_{\text{Na}}^{\text{Al}} > \alpha_{\text{Sr}}^{\text{Al}} \approx \alpha_{\text{Mg}}^{\text{Al}} > \alpha_{\text{K}}^{\text{Al}} \approx \alpha_{\text{Cs}}^{\text{Al}} > \alpha_{\text{Ba}}^{\text{Al}} \approx \alpha_{\text{Rb}}^{\text{Al}}$$

is more poorly defined than for mud samples, largely because α^{Al} values vary more erratically. This is particularly true for elements associated with phyllosilicates (Mg, K, Rb, and particularly Cs). Ca is commonly more depleted than Na in sands, reflecting the greater lability of Ca feldspar relative to alkali feldspar [Nesbitt *et al.*, 1996; White *et al.*, 2001]. The contrasting mobility pattern of Na and Ca in different samples requires that their apparent bulk-sediment mobility α^{Al} is controlled not only by the elements' atomic properties but by the hosting detrital minerals as well.

6.4. Contrasting Weathering Intensity on Opposite Rift-Shoulder Flanks: The Tectonic Effect

[56] Sediment composition is invariably controlled by numerous interplaying factors in nature. When using a natural laboratory, we thus need to select the appropriate setting to reduce the complexity of the system, in order to ideally isolate one single factor and assess its relative incidence. By comparing the compositional fingerprints of sediment produced on opposite flanks of the same tectonic structure, for instance, we can minimize the effect of several variables, including differences in bedrock lithology at the headwaters. In order to evaluate the impact of different weathering intensity on opposite sides of the Kivu-Tanganyika rift shoulder, we thus systematically compared the mineralogy and geochemistry of mud samples collected in adjacent drainage basins across the catchment divide, all the way from SW Burundi to NE Rwanda (Table 1). The investigated pairs are (western Congo side versus eastern Kagera side): Murembwe versus Ruvyironza, Mugere and Ruzibazi versus Mubarazi, Rusizi tributaries versus Akanyaru and Ruvubu headwaters, Karundura versus Nyabarongo headwaters, and Koko versus Gicyie (Figure 2).

[57] In all of these five pairs, feldspars and particularly plagioclase are observed to be less abundant and the kaolinite/illite ratio invariably higher on the Kagera side. Smectite occurs only on the Congo side (Figure 4), where chlorite is more frequently detected and Fe oxyhydroxides are less abundant. The CIA and with a few exceptions α^{Al} indices (similar $\alpha_{\text{Sr}}^{\text{Al}}$

and $\alpha_{\text{Ba}}^{\text{Al}}$ in the first and third pairs; similar $\alpha_{\text{Ca}}^{\text{Al}}$ in the fourth pair; slightly lower $\alpha_{\text{K}}^{\text{Al}}$ in Gicyie mud reflecting higher phyllosilicate/feldspar ratio in the Gishwati Province) consistently indicate more extensive weathering in mountain catchments on the Kagera side of the Kivu-Tanganyika rift shoulder (Figure 8). Besides local heterogeneous distribution of parent lithologies and other asymmetries including overall greater preservation of higher tectono-stratigraphic levels of the uplifted crust on the outer rift flank, mineralogical and geochemical parameters thus coherently document more extensive weathering in the headwaters of diverse Kagera branches along the Nile side of the divide than along the Congo side. Such systematic compositional differences reflect weaker and/or less prolonged chemical weathering along the drier and steeper inner flank of the shoulder facing the Kivu-Tanganyika rift axis. Along the outer flank, exposed to humid masses blown from the Indian Ocean by the southeasterly monsoon that represents the principal moisture source for precipitation, erosion rates are low enough to allow development of thick ferrallitic soils on the central plateau and rolling hills of Burundi and Rwanda.

6.5. Weathering From Mountain Soils to Lowland Floodplains: The Transport Effect

[58] Close inspection of mineralogical and geochemical trends in diverse catchments helps us to understand where and by which processes chemical weathering occurs. We can thus evaluate the relative incidence of parent-rock alteration during pedogenesis at the very beginning of the sedimentary cycle, versus later progressive modification during stepwise downstream transport. If we first contrast rill muds collected at the two main sources of the Kagera-Nile in Burundi and Rwanda with muds in diverse headwater tributaries of the Nyabarongo and Ruvubu Rivers, then we do not observe significant differences in composition, kaolinite/smectite ratios, or chemical weathering indices. This suggests that mud removed mechanically from superficial soil layers is virtually the same as that progressively collected by tributaries and carried in suspension by main rivers downstream.

[59] If we next analyze mineralogical and geochemical indices in eight major catchments, including all major branches of the Kagera River on the Nile side of the divide and the Rusizi and Malagarasi basins on the Congo side (Figure 2), then we see that none of them displays a further significant increase in weathering downstream. Changes in mud geochemistry are chiefly accounted for by successive contributions

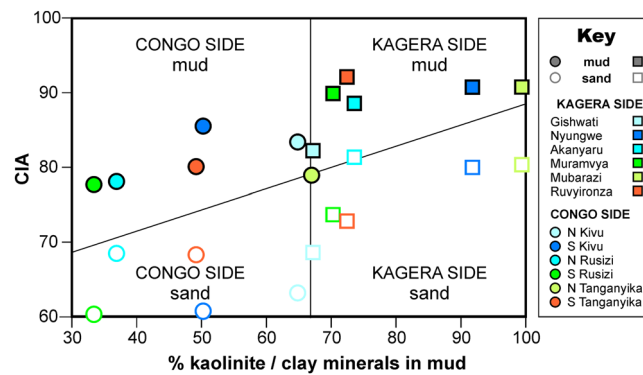


Figure 8. Contrasting weathering conditions on opposite rift-shoulder flanks. Clay mineralogy and chemical indices consistently reveal more intense weathering in hot-humid forested highlands on the eastern Kagera-Nile side of the divide, where slopes are milder, and time for weathering longer, than along the steep inner flank and drier axis of the rift (Congo side). Note that CIA values are invariably higher for mud samples than for corresponding sand samples.

from tributaries through the Kagera basin, where weathering is strongest in humid highlands. Downstream depletion in mobile elements is chiefly caused by extensive recycling of Karagwe-Ankole quartzose meta-sediments across eastern Burundi and Rwanda. The kaolinite/illite ratio decreases in fact from Kagera headwaters to the lower course, where appearance of significant smectite reflects local contribution from drier savannah lowlands (Figure 4). Downstream the Nyabarongo, increasing plagioclase, decreasing Fe oxyhydroxides, and moderate but coherent trends displayed by most chemical indices consistently suggest that fresher material is added to the river by tributaries draining drier areas. In the Malagarasi, Ruvubu, Mubarazi, and Ruvyironza basins, where muds are largely recycled from meta-sedimentary sources, mineralogical and geochemical trends are less clear but also suggest decreasing rather than increasing weathering downstream. The compositional trends shown by Mukungwa and Rusizi muds, both indicating increasing weathering downstream, are fully accounted for by dominant supply from major tributaries draining humid rift highlands in the Gishwati and Kibira Forests. All mineralogical and geochemical parameters thus consistently indicate that leaching of soluble cations is more effective in well-drained udic soils of humid rift highlands than in poorly drained ustic soils of drier savannah lowlands. The incidence of weathering during temporary storage of sediment, as observed instead in the vast floodplains of the huge Amazon and Ganga-Brahmaputra [Moquet *et al.*, 2011; Lupker *et al.*, 2012], is negligible in the smaller catchments of the East African Rift.

7. Weathering Versus Recycling

[60] Any large drainage basin includes ancient clastic strata that have undergone more than one

sedimentary cycle. The mineralogical and chemical composition of newly produced detritus thus reflects the present weathering conditions as well as the effects of such previous weathering and diagenetic histories. Isolating the climatic signal from such composite record is perhaps the most daring task in sedimentary petrology and geochemistry [Cox *et al.*, 1995; Gaillardet *et al.*, 1999]. The great advantage of a study based on modern fluvial sediments is that the incidence of recycling can be known a priori. Our samples were in fact expressly collected in river catchments where only metamorphic or igneous basement rocks are exposed (and recycling is consequently negligible; e.g., Nyungwe Province) or on the contrary dominated by very low grade to low-grade quartzose meta-sediments (Eastern and Western Domains) and entirely comprised within rift-related Neogene basins (Lake Albert Province). Nevertheless, by contrasting first-cycle plutoniclastic and metamorphiclastic equatorial sediments with detritus entirely recycled from quartzose meta-sediments or syn-rift sands, we did not observe any tell-tale behavior exclusively associated with either weathering or recycling displayed by any specific chemical element. Depletion in alkali and alkaline-earth metals is not necessarily the imprint of weathering. It is equally displayed by quartzose polycyclic detritus produced even in hyper-arid deserts like the Sahara [Garzanti *et al.*, 2006; Padoan *et al.*, 2011].

[61] The best way we found to tackle such challenging problem is to confront indices such as the WIP, which decreases linearly if quartz is added to the sediment, with other weathering indices virtually unaffected by quartz dilution such as the CIA or α^{Al} values. We thus compared and could partly discriminate among the effects of pure weathering as displayed by quartz-poor first-cycle muds and

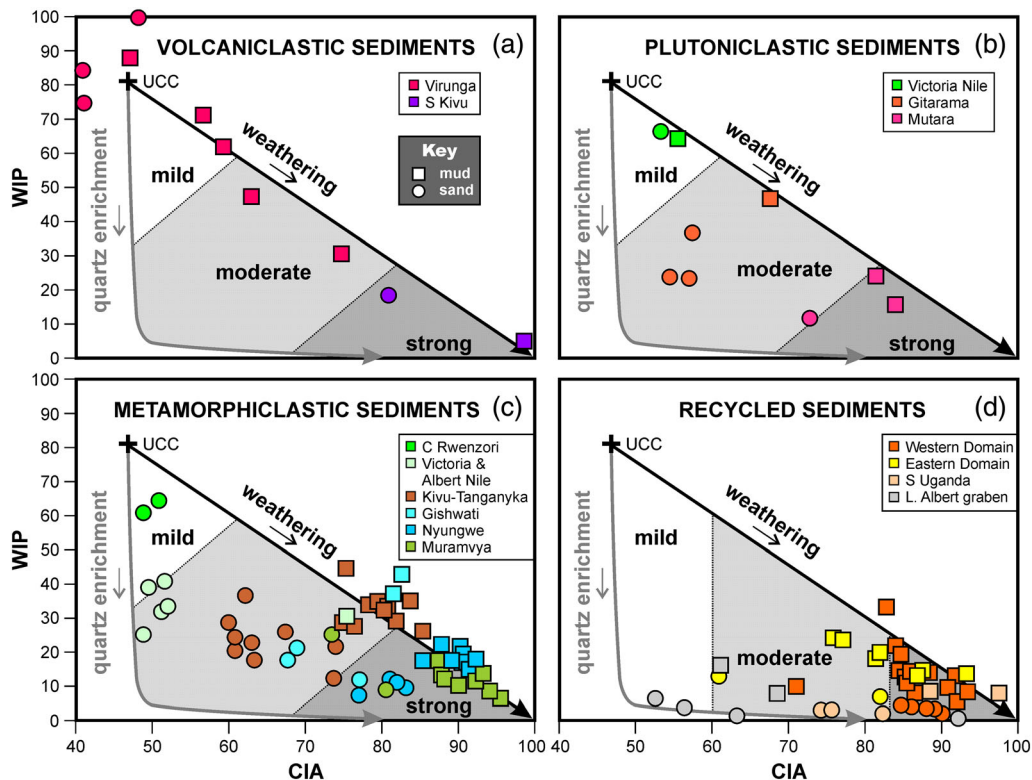


Figure 9. Discriminating first-cycle and polycyclic sediments with chemical indices. Because quartz dilution affects strongly WIP but not CIA, the CIA/WIP plot readily reveals quartz enrichment in sediments. The relationship between CIA and WIP is linear for first-cycle muds as well as for quartz-poor volcaniclastic sands (a), whereas with increasing weathering intensity, quartz enrichment causes a marked decrease of WIP in plutoniclastic and metamorphiclastic sands (b, c). Sediments recycled from quartzose sediments and meta-sediments display low WIP even where weathering is limited, as revealed by low CIA (d). Sands, largely resulting from physical erosion, invariably display lower CIA than muds, the ultimate product of chemical weathering.

volcaniclastic sands, of pure quartz dilution as displayed by recycled sands produced by physical processes in weathering-limited conditions, and of quartz enrichment as displayed by weathered first-cycle sands produced by chemical processes in transport-limited conditions (Figure 9). The effect of quartz dilution is most easily detected in drier regions, where recycling is indicated by very low WIP in spite of relatively low CIA but progressively blurred with increasing weathering intensity. In hot hyperhumid regions, CIA is very high and WIP very low for both first-cycle and polycyclic sediments, and the recycling problem thus harder to solve. However, for any given CIA, the WIP remains lower for polycyclic mud and approaches 0 for recycled sand (Figure 9D).

8. Conclusion

[62] By integrating a variety of mineralogical and geochemical datasets, we have critically appraised the effect of different factors controlling sediment composition across equatorial Africa and in

particular the mark of chemical weathering impressed by hot humid climate and consequently intense ferrallitic pedogenesis. Muds collected along the East African Rift in the Nile and Congo headwaters and derived from different bedrock lithologies consistently display depletion in mobile alkali and alkaline-earth metals. Element removal is observed to be extreme for Na and Ca, strong for Sr, moderate for Mg and K, minor for Ba and Rb, and negligible for Cs. Such order of apparent bulk-sediment mobility is coherent with the degree into which these elements are partitioned in plagioclase, K-feldspar, and primary or secondary phyllosilicates. Conversely, $^{87}\text{Sr}/^{86}\text{Sr}$ ratios, $^{143}\text{Nd}/^{144}\text{Nd}$ ratios, and Sm-Nd t_{DM} model ages of river muds proved to be insensitive to weathering and provide a faithful integrated signature of the geological history of each drainage basin.

[63] Kaolinite is by far the most abundant clay mineral in muds produced in rain-forest highlands of Burundi and Rwanda, reflecting intense and prolonged leaching of mobile cations in nitisols

developed in udic isothermic/isomesic regime. Smectite forms instead in drier and poorly drained savannah lowlands characterized by ferralsols or lixisols developed in ustic iso-hyperthermic regime. Kaolinite is dominant also in volcanoclastic mud produced in the South Kivu field, where weathering is much more intense than in the rain shadow of the Virunga volcanoes. No significant mineralogical or geochemical differences are observed between rill mud derived from superficial soil layers and mud carried in suspension by rivers downstream. No downstream increase in weathering indices can be ascribed to progressive maturation during stepwise transport in any of the eight major drainage basins studied. Mineralogical and geochemical parameters consistently indicate that weathering is more intense in hot humid highlands along the eastern side of the Nile-Congo divide than along the steeper and drier inner rift-shoulder flank. Weathering is least in dry areas of western Uganda, including the central Rwenzori massif where physical erosion prevails and the northern Lake Albert graben where detritus is largely recycled from syn-rift Neogene deposits. The CIA and WIP indices are both low in such polycyclic sediments, an apparent discrepancy that reveals the incidence of recycling and thus offers a solution to one of the thorniest problems in sedimentary geochemistry.

Acknowledgments

[64] The article greatly benefited from reviews by Robert Cullers and a conspicuous number of anonymous reviewers. We heartily thank Paolo Censi, Jérôme Gaillardet, and Michele Lustrino for discussion of diverse geochemical aspects; Fabio Scarciglia and Silvia Chersich for advice on pedogenic features; Stijn Dewaele, Max Fernandez-Alonso, and Luc Tack for geological information and publications; Luigi Marinoni for assistance in XRD analyses; and drivers Bob Mpanga, Isaac, and Mugabi Baghenda and singer José Kamilyon for company during our joyous sampling campaigns.

References

- Abdelsalam, G. M., J. P. Liégeois, and R. J. Stern (2002), The Saharan Metacraton. *J. African Earth Sci.*, *34*, 119–136.
- Allègre, C. J., B. Dupré, P. Nègre, and J. Gaillardet (1996), Sr-Nd-Pb isotope systematics in Amazon and Congo River systems: Constraints about erosion processes. *Chem. Geol.*, *131*, 93–112.
- Andò, S., E. Garzanti, M. Padoan, and M. Limonta (2012), Corrosion of heavy minerals during weathering and diagenesis: A catalog for optical analysis. *Sedim. Geol.*, *280*, 165–178.
- Appel, P., V. Schenk, and A. Schumann (2005), P-T path and metamorphic ages of pelitic schists at Murchison Falls, NW Uganda: Evidence for a Pan-African tectonometamorphic event in the Congo Craton. *Eur. J. Miner.*, *17*, 655–664.
- Baudet, D., M. Hanon, E. Lemonne, and K. Theunissen (1988), Lithostratigraphie du domaine sédimentaire de la chaîne Kibarienne au Rwanda. *Ann. Soc. Géol. Belgique*, *112*, 225–246.
- Bell, K., and J. L. Powell (1969), Strontium isotopic studies of alkaline rocks: The potassium rich lavas of the Birunga and Toro-Ankole Regions, East and Central Equatorial Africa. *J. Petrol.*, *10*, 536–572.
- Biscaye, P. E. (1965), Mineralogy and sedimentation of recent deep-sea clay in the Atlantic Ocean and adjacent seas and oceans. *Geol. Soc. Am. Bull.*, *76*, 803–832.
- Borges, J., and Y. Huh (2007), Petrography and chemistry of the bed sediments of the Red River in China and Vietnam: Provenance and chemical weathering. *Sedim. Geol.*, *194*, 155–168.
- Bouchez, J., M. Lupker, J. Gaillardet, C. France-Lanord, and L. Maurice (2011a), How important is it to integrate riverine suspended sediment chemical composition with depth? Clues from Amazon River depth-profiles. *Geochim. Cosmochim. Acta*, *75*, 6955–6970.
- Bouchez, J., J. Gaillardet, C. France-Lanord, L. Maurice, and P. Dutra-Maia (2011b), Grain size control of river suspended sediment geochemistry: clues from Amazon River depth profiles. *Geochem. Geophys. Geosyst.*, *12*, Q03008, doi:10.1029/2010GC003380.
- Braun, J. J., M. Pagel, J. P. Muller, P. Bilong, A. Michard, and B. Guillet (1990), Cerium anomalies in lateritic profiles. *Geochim. Cosmochim. Acta*, *54*, 781–795.
- Brinckmann, J., B. Lehmann, and F. Timm (1994), Proterozoic gold mineralization in NW Burundi. *Ore Geol. Rev.*, *9*, 85–103.
- Brown, E. T., J. M. Edmond, G. M. Raisbeck, D. L. Bourlès, F. Yiou, and C. I. Measures (1992), Beryllium isotope geochemistry in tropical river basins. *Geochim. Cosmochim. Acta*, *56*, 1607–1624.
- Brown, D. J., P. A. Helmke, and M. K. Clayton (2003), Robust geochemical indices for redox and weathering on a granitic laterite landscape in central Uganda. *Geochim. Cosmochim. Acta*, *67*, 2711–2723.
- Buchwaldt, R., T. Toulkeridis, W. Todt, and E. K. Ucakuwun (2008), Crustal age domains in the Kibaran belt of SW-Uganda: Combined zircon geochronology and Sm-Nd isotopic investigation. *J. Afr. Earth Sci.*, *51*, 4–20.
- Büttner, A., I. C. Kleinhanns, D. Rufer, J. C. Hunziker, and I. M. Villa (2005), Magma generation at the easternmost section of the Hellenic arc: Hf, Nd, Pb and Sr isotope geochemistry of Nisyros and Yali volcanoes (Greece). *Lithos*, *83*, 29–46.
- Canfield, D. E. (1997), The geochemistry of river particulates from the continental USA: Major elements. *Geochim. Cosmochim. Acta*, *61*, 3349–3365.
- Chamley, H. (1989), Clay sedimentology. 623p. Springer, Berlin.
- Cox, R., D. R. Lowe, and R. L. Cullers (1995), The influence of sediment recycling and basement composition on evolution of mudrock chemistry in the southwestern United States. *Geochim. Cosmochim. Acta*, *59*, 2919–2940.
- Deblond, A., L. E. Punzalan, A. Boven, and L. Tack (2001), The Malagarazi Supergroup of southeast Burundi and its correlative Bukoba Supergroup of northwest Tanzania: Neo- and Mesoproterozoic chronostratigraphic constraints from Ar-Ar ages on mafic intrusive rocks. *J. Afr. Earth Sci.*, *29*, 313–328.

- De Mulder, M., J. Hertogen, S. Deutsch, and L. André (1986), The role of crustal contamination in the potassic suite of the Karisimbi volcano (Virunga, African Rift Valley). *Chem. Geol.*, *57*, 117–136.
- Drever, J. I. (1994), The effect of land plants on weathering rates of silicate minerals. *Geochim. Cosmochim. Acta*, *58*, 2325–2332.
- Duchesne, J. C., J. P. Liégeois, A. Deblond, and L. Tack (2004), Petrogenesis of the Kabanga-Musongati layered mafic-ultramafic intrusions in Burundi (Kibaran Belt): Geochemical, Sr-Nd isotopic constraints and Cr-Ni behaviour. *J. Afr. Earth Sci.*, *39*, 133–145.
- Dupré, B., J. Gaillardet, D. Rousseau, and C. J. Allègre (1996), Major and trace elements of river-borne material: The Congo Basin. *Geochim. Cosmochim. Acta*, *60*, 1301–1321.
- Ebinger, C. J. (1989), Tectonic development of the western branch of the East-African rift system. *Geol. Soc. Am. Bull.*, *101*, 885–903.
- Ebinger, C., and T. Furman (2003), Geodynamical setting of the Virunga volcanic province. *Acta Vulc.*, *14*, 1–8.
- Edmond, J. M., M. R. Palmer, C. I. Measures, E. T. Brown, and Y. Huh (1996), Fluvial geochemistry of the eastern slope of the northeastern Andes and its foredeep in the drainage of the Orinoco in Colombia and Venezuela. *Geochim. Cosmochim. Acta*, *60*, 2949–2976.
- Fernandez-Alonso, M. (2007), Geological Map of the Mesoproterozoic Northeastern Kibara Belt, 1:500,000. Royal Museum for Central Africa, Tervuren (Belgium).
- Fernandez-Alonso, M., and K. Theunissen (1998), Airborne geophysics and geochemistry provide new insights in the intracratonic evolution of the Mesoproterozoic Kibaran belt (Central Africa). *Geol. Mag.*, *135*, 203–216.
- Fernandez-Alonso, M., J. Lavreau, and J. Klerkx (1986), Geochemistry and geochronology of the Kibaran granites in Burundi, Central Africa: Implications for the Kibaran Orogeny. *Chem. Geol.*, *57*, 234–217.
- Fernandez-Alonso, M., H. Cutten, B. De Waele, L. Tack, A. Tahon, D. Baudet, and S. D. Barritt (2012), The Mesoproterozoic Karagwe-Ankole Belt (former NE Kibaran belt): The result of prolonged extensional intracratonic basin development punctuated by two short-lived far-field compressional events. *Precambrian Res.*, *216/219*, 63–86.
- Furman, T., and D. Graham (1999), Erosion of lithospheric mantle beneath the East African Rift system: Geochemical evidence from the Kivu volcanic province. *Lithos*, *48*, 237–262.
- Gaillardet, J., B. Dupré, and C. J. Allègre (1999), Geochemistry of large river suspended sediments: Silicate weathering or recycling tracer? *Geochim. Cosmochim. Acta*, *63*, 4037–4051.
- Gaillardet, J., J. Viers, and B. Dupré (2003), Trace elements in river waters, in Surface and ground water, weathering, erosion and soils, edited by J.I. Drever, vol. 5, pp. 225–272, in Treatise on geochemistry, edited by H.D. Holland and K.K. Turekian, Elsevier, Pergamon.
- Garzanti, E., and S. Andò, S. (2007), Plate tectonics and heavy-mineral suites of modern sands, in Heavy Minerals in Use, edited by M.A. Mange and D.T. Wright, Developments in Sedimentology Series, v. 58, pp. 741–763, Elsevier, Amsterdam.
- Garzanti, E., G. Vezzoli, S. Andò, and G. Castiglioni (2001), Petrology of rifted-margin sand (Red Sea and Gulf of Aden, Yemen). *J. Geol.*, *109*, 277–297.
- Garzanti, E., S. Andò, G. Vezzoli, A. Ali Abdel Megid, and A. El Kammar (2006), Petrology of Nile River sands (Ethiopia and Sudan): Sediment budgets and erosion patterns. *Earth Planet. Sci. Lett.*, *252*, 327–341.
- Garzanti, E., S. Andò, and G. Vezzoli (2008), Settling-equivalence of detrital minerals and grain-size dependence of sediment composition. *Earth Planet. Sci. Lett.*, *273*, 138–151.
- Garzanti, E., S. Andò, C. France-Lanord, G. Vezzoli, P. Censi, V. Galy, Y. Najman (2010), Mineralogical and chemical variability of fluvial sediments. 1. Bedload sand (Ganga-Brahmaputra, Bangladesh). *Earth Planet. Sci. Lett.*, *299*, 368–381.
- Garzanti, E., S. Andò, C. France-Lanord, V. Galy, P. Censi, and P. Vignola (2011), Mineralogical and chemical variability of fluvial sediments. 2. Suspended-load silt (Ganga-Brahmaputra, Bangladesh). *Earth Planet. Sci. Lett.*, *302*, 107–120.
- Garzanti, E., A. Resentini, G. Vezzoli, S. Andò, M. Malusà, and M. Padoan (2012), Forward compositional modelling of Alpine orogenic sediments. *Sedim. Geol.*, *280*, 149–164.
- Garzanti, E., M. Padoan, S. Andò, A. Resentini, G. Vezzoli, and M. Lustrino (in review), Weathering at the equator: petrology and geochemistry of East African Rift sands. *J. Geol.*
- Goldstein, S. J., and S. B. Jacobsen (1988), The Nd and Sr isotopic systematics of river water suspended material: Implications for crustal evolution. *Earth Planet. Sci. Lett.*, *87*, 249–265.
- Goldstein, S. L., R. K. O’Nions, and P. J. Hamilton (1984), A Sm-Nd isotopic study of atmospheric dusts and particulates from major river systems. *Earth Planet. Sci. Lett.*, *70*, 221–236.
- Haley, B. A., G. P. Klinkhammer, and J. McManus (2004), Rare earth elements in pore waters of marine sediments. *Geochim. Cosmochim. Acta*, *68*, 1265–1279.
- Hildebrand, K. (1984), Étude des complexes granito-gneissiques de Cymbili, Mara et Mutara, République Rwandaise (Afrique Centrale). PhD Thesis, University of Quebec at Chicoutimi, 249 pp.
- Holmes, A., and F. Harwood (1937), The petrology of the volcanic area of Bufumbira. *Memoirs of the Geological Survey of Uganda* 3 (2), 300 pp.
- Hu, Z., and S. Gao (2008), Upper crustal abundances of trace elements: A revision and update. *Chem. Geol.*, *253*, 205–221.
- Ilunga, L. (1991), Morphologie, volcanisme et sédimentation dans le rift du Sud-Kivu. *Bull. Soc. Géogr. Liège*, *27*, 209–228.
- Johnsson, M. J. (1993), The system controlling the composition of clastic sediments, in Processes Controlling the Composition of Clastic Sediments, edited by M.J. Johnsson and A. Basu, Special Papers 284, pp. 1–19, Geol. Soc. Am..
- Klerkx, J., J. P. Liégeois, J. Lavreau, and W. Claessen (1987), Crustal evolution of northern Kibaran belt in eastern and central Africa, in Proterozoic Crustal Evolution, edited by A. Kroner, Geodynamics Series 17, pp. 217–233, Am. Geophys. Union.
- Kottek, M., J. Grieser, C. Beck, B. Rudolf, and F. Rubel (2006), World Map of the Köppen-Geiger climate classification updated. *Meteorologische Zeitung*, *15*, 259–263.
- Kronberg, B. I., H. W. Nesbitt, and W. S. Fyfe (1987), Mobilities of alkalis, alkaline earths and halogens during weathering. *Chem. Geol.*, *60*, 41–49.
- Lehmann, B., S. Nakai, A. Höhndorf, J. Brinckmann, P. Dulski, U. F. Hein, and A. Masuda (1994), REE mineralization at Gakara, Burundi: Evidence for anomalous upper mantle in the western Rift Valley. *Geochim. Cosmochim. Acta*, *58*, 985–992.
- Link, K., D. Koehn, M. G. Barth, J. V. Tiberindwa, E. Barifaijo, K. Aanyu, and S. F. Foley (2010), Continuous cratonic crust

- between the Congo and Tanzania blocks in western Uganda. *Int. J. Earth Sci.*, *99*, 1559–1573.
- Lugmair, G. W., N. B. Scheinin, and K. Marti (1975), Sm-Nd age and history of Apollo 17 basalt 7505: Evidence for early differentiation of the lunar exterior. Proc. 6th Lunar Science Conference, pp. 1419–1429.
- Lupker, M., C. France-Lanord, J. Lavé, J. Bouchez, V. Galy, F. Métyvier, J. Gaillardet, B. Lartiges, and J. L. Mugnier (2011), A Rouse-based method to integrate the chemical composition of river sediments: Application to the Ganga basin. *J. Geophys. Res.*, *116*, F04012, doi:10.1029/2010JF001947.
- Lupker, M., C. France-Lanord, V. Galy, J. Lavé, J. Gaillardet, A.P. Gajurel, C. Guilmette, M. Rahman, S.K. Singh, and R. Sinha (2012), Predominant floodplain over mountain weathering of Himalayan sediments (Ganga basin). *Geochim. Cosmochim. Acta*, *84*, 410–432.
- Maier, W. D., S. J. Barnes, D. Bandyayera, T. Livesey, C. Li, and E. Ripley (2008), Early Kibaran rift-related mafic-ultramafic magmatism in western Tanzania and Burundi: Petrogenesis and ore potential of the Kapalagulu and Musongati layered intrusions. *Lithos*, *101*, 24–53.
- Martin, J. M., and M. Meybeck (1979), Elemental mass-balance of material carried by major world rivers. *Marine Chem.*, *7*, 173–206.
- Martin, J. M., A. J. Thomas, and R. Van Grieken (1978), Trace element composition of Zaire suspended sediments. *Netherlands J. Sea Res.*, *12*, 414–420.
- McDonough, W. F., and S. S. Sun (1995), The composition of the Earth. *Chem. Geol.* *120*, 223–253.
- McLennan, S. M. (1989), Rare earth elements in sedimentary rocks: Influence of provenance and sedimentary processes. *Rev. Miner. Geochem.*, *21*, 169–200.
- McLennan, S. M. (2001), Relationships between the trace element composition of sedimentary rocks and upper continental crust. *Geochim. Geophys. Geosyst.*, *2*, 2000GC000109.
- Middleburg, J. J., C. H. van der Weijden, and J. R. W. Woittiez (1988), Chemical processes affecting the mobility of major, minor and trace elements during weathering of granitic rocks. *Chem. Geol.*, *68*, 253–273.
- Moeyersons, J. (2003), The topographic thresholds of hillslope incisions in southwestern Rwanda. *Catena*, *50*, 381–400.
- Moeyersons, J., P. Tréfois, J. Lavreau, D. Alimasi, I. Badriyo, B. Mitima, M. Mundala, D. O. Munganga, and L. Nahimana (2004), A geomorphological assessment of landslide origin at Bukavu, Democratic Republic of the Congo. *Eng. Geol.*, *72*, 73–87.
- Moore, D. M., and R. C. Reynolds (1989), X-ray Diffraction and the Identification and Analysis of Clay Minerals. , 332 pp. Oxford Univ. Press, New York.
- Moquet, J. S., A. Crave, J. Viers, P. Seyler, E. Armijos, L. Bourrel, E. Chavari, C. Lagane, A. Laraque, W.S. Lavado Casimiro, et al. (2011), Chemical weathering and atmospheric/soil CO₂ uptake in the Andean and foreland Amazon basins. *Chem. Geol.*, *287*, 1–26.
- Nägler, T. F., and B. S. Kamber (1996), A new silicate dissolution procedure for isotope studies on garnet and other rock forming minerals. *Schweiz. miner. petrogr. Mitt.*, *76*, 75–80.
- Nägler, T. F., and J. D. Kramers (1998), Nd isotopic evolution of the upper mantle during the Precambrian: Models, data and the uncertainty of both. *Precambrian Res.*, *91*, 233–252.
- Nagudi, B., C. Koeberl, and G. Kurat (2003), Petrography and geochemistry of the Singo granite, Uganda, interpretations and implications for its origin. *J. Afr. Earth Sci.*, *36*, 73–87.
- Négrel, P., C. J. Allègre, B. Dupré, and E. Lewin (1993), Erosion sources determined by inversion of major and trace element ratios in river water: The Congo Basin case. *Earth Planet. Sci. Lett.*, *120*, 59–76.
- Nesbitt, H. W., and G. Markovics (1997), Weathering of granodioritic crust, long-term storage of elements in weathering profiles, and petrogenesis of clastic sediments. *Geochim. Cosmochim. Acta*, *61*, 1653–1670.
- Nesbitt, H. W., and G. M. Young (1982), Early Proterozoic climates and plate motions inferred from major element chemistry of lutites. *Nature*, *299*, 715–717.
- Nesbitt, H. W., G. Markovics, and R. C. Price (1980), Chemical processes affecting alkalis and alkali earths during continental weathering. *Geochim. Cosmochim. Acta*, *44*, 1659–1666.
- Nesbitt, H. W., G. M. Young, S. M. McLennan, and R. R. Keays (1996), Effects of chemical weathering and sorting on the petrogenesis of siliciclastic sediments, with implications for provenance studies. *J. Geol.*, *104*, 525–542.
- Nizeyimana, E., and T. J. Bicki (1992), Soil and soil-landscape relationships in the north central region of Rwanda, East-Central Africa. *Soil Sci.*, *153*, 225–236.
- Nyakairu, G. W. A., and C. Koeberl (2001), Mineralogical and chemical composition and distribution of rare earth elements in clay-rich sediments from central Uganda. *Geochem. J.*, *35*, 13–28.
- Nyakairu, G. W. A., C. Koeberl, and H. Kurzweil (2001), The Buwambo kaolin deposit in central Uganda: Mineralogical and chemical composition. *Geochem. J.*, *35*, 245–256.
- Padoan, M., E. Garzanti, Y. Harlavan, and I. M. Villa (2011), Tracing Nile sediment sources by Sr and Nd isotope signatures (Uganda, Ethiopia, Sudan). *Geochim. Cosmochim. Acta*, *75*, 3627–3644.
- Parker, A. (1970), An index of weathering for silicate rocks. *Geol. Mag.*, *107*, 501–504.
- Pohl, W. (1994), Metallogeny of the northeastern Kibara belt, Central Africa—Recent perspectives. *Ore Geol. Rev.*, *9*, 105–130.
- Price, J. R., and M. A. Velbel (2003), Chemical weathering indices applied to weathering profiles developed on heterogeneous felsic metamorphic parent rocks. *Chem. Geol.*, *202*, 397–416.
- Ring, U. (2008), Extreme uplift of the Rwenzori Mountains in the East African Rift, Uganda: Structural framework and possible role of glaciations. *Tectonics*, *27*, TC4018, doi:10.1029/2007TC002176.
- Rogers, N. W., M. De Mulder, and C. J. Hawkesworth (1992), An enriched mantle source for potassic basanites: Evidence from Karisimbi volcano, Virunga volcanic province, Rwanda. *Contrib. Miner. Petrol.*, *111*, 543–556.
- Rogers, N. W., D. James, S. P. Kelley, and M. De Mulder (1998), The generation of potassic lavas from the eastern Virunga Province, Rwanda. *J. Petrol.*, *39*, 1223–1247.
- Rosenthal, A., S. F. Foley, D. G. Pearson, G. M. Nowell, and S. Tappe (2009), Petrogenesis of strongly alkaline primitive volcanic rocks at the propagating tip of the western branch of the East African Rift. *Earth Planet. Sci. Lett.*, *284*, 236–248.
- Scarciglia, F., P. Tuccimei, A. Vacca, D. Barca, I. Pulice, R. Salzano, and M. Soligo (2011), Soil genesis, morphodynamic processes and chronological implications in two soil transects of SE Sardinia, Italy: Traditional pedological study coupled with laser ablation ICP-MS and radionuclide analyses. *Geoderma*, *162*, 39–64.
- Schlüter, T. (2008), Geological atlas of Africa. 307 pp. Springer Verlag, Berlin.
- Shao, J., S. Yang, and C. Li (2012), Chemical indices (CIA and WIP) as proxies for integrated chemical weathering in China:

- Inferences from analysis of fluvial sediments. *Sedim. Geol.*, 265-266, 110–120.
- Shiller, A. M. and D. M. Frilot (1996), The geochemistry of gallium relative to aluminium in Californian streams. *Geochim. Cosmochim. Acta*, 60, 1323–1328.
- Soil map of Rwanda (1994), Laboratory of Soil Science, University of Ghent, scale 1:50,000, <http://zadeh.ugent.be/rwanda>
- Soreghan, M. J., and A. S. Cohen (1993), The effects of basin asymmetry on sand composition: Examples from Lake Tanganyika, Africa, in *Processes Controlling the Composition of Clastic Sediments*, edited by M.J. Johnsson and A. Basu, Spec. Pap. 284, pp. 285–301, Geol. Soc. Am.
- Stallard, R. F. (1988), Weathering and erosion in the humid tropics, in *Physical and Chemical Weathering in Geochemical Cycles*, edited by A. Lerman and M. Meybeck, NATO Science Series C, Mathematical and physical sciences, 251, pp. 225–246, Kluwer, Dordrecht.
- Sutcliffe, J. V. and Y. P. Parks (1999), The hydrology of the Nile. *Int. Ass. Hydrol. Sci., Spec. Publ. 5*, 179 p.
- Tack, L., J. P. Liégeois, A. Deblond, and J. C. Duchesne (1994), Kibaran A-type granitoids and mafic rocks generated by two mantle sources in a late orogenic setting (Burundi). *Precambrian Res.*, 68, 323–356.
- Tack, L., M. T. D. Wingate, B. De Waele, J. Meerte, E. Belousova, B. Griffin, A. Tahon, and M. Fernandez-Alonso (2010), The 1375 Ma “Kibaran event” in Central Africa: Prominent emplacement of bimodal magmatism under extensional regime. *Precambrian Res.*, 180, 63–84.
- Tauler, E., J. A. Proenza, S. Galí, J. F. Lewis, M. Labrador, E. García-Romero, M. Suarez, F. Longo, and G. Bloise (2009), Ni-sepiolite-falcondoite in garnierite mineralization from the Falcondo Ni-laterite deposit, Dominican Republic. *Clay Miner.*, 44, 435–454.
- Taylor, R. G., and K. W. F. Howard (1999), The influence of tectonic setting on the hydrological characteristics of deeply weathered terrains: Evidence from Uganda. *J. Hydrol.*, 218, 44–71.
- Taylor, R. G., L. Mileham, C. Tindimugaya, and L. Mwebembezi (2009), Recent glacial recession and its impact on alpine riverflow in the Rwenzori Mountains of Uganda. *J. Afr. Earth Sci.*, 55, 205–213.
- Taylor, S. R., and S. M. McLennan (1985), *The Continental Crust: Its Composition and Evolution*. 312p. Blackwell Scientific, Boston.
- Taylor, S. R., and S. M. McLennan (1995), The geochemical evolution of the continental crust. *Rev. Geophys.*, 33, 241–265.
- Velbel, M. A. (1993), Temperature dependence of silicate weathering in nature: How strong a negative feedback on long-term accumulation of atmospheric CO₂ and global greenhouse warming. *Geology*, 21, 1059–1062.
- Velde, B. (1995), *Origin and Mineralogy of Clays*. 371p. Springer, Berlin.
- Viers, J., B. Dupré, and J. Gaillardet (2009), Chemical composition of suspended sediments in world rivers: New insights from a new database. *Sci. Total Environ.*, 407, 853–868.
- Vollmer, R., and M. J. Norry (1983), Possible origin of K-rich volcanic rocks from Virunga, East Africa, by metasomatism of continental crustal material: Pb, Nd and Sr isotopic evidence. *Earth Planet. Sci. Lett.*, 64, 374–386.
- Young, G. M., and H. W. Nesbitt (1998), Processes controlling the distribution of Ti and Al in weathering profiles, siliciclastic sediments and sedimentary rocks. *J. Sedim. Res.*, 68, 448–455.
- Wasserburg, G. J., S. B. Jacobsen, D. J. DePaolo, M. T. McCulloch, and T. Wen (1981), Precise determination of Sm/Nd ratios, Sm and Nd isotopic abundances in standard solutions. *Geochim. Cosmochim. Acta*, 45, 2311–2323.
- White, A. F., and A. E. Blum (1995), Effects of climate on chemical weathering in watersheds. *Geochim. Cosmochim. Acta*, 59, 1729–1747.
- White, A. F., T. D. Bullen, M. S. Schulz, A. E. Blum, T. G. Huntington, and N. E. Peters (2001), Differential rates of feldspar weathering in granitic regoliths. *Geochim. Cosmochim. Acta*, 65, 847–869.
- Wilson, M. J. (1999), The origin and formation of clay minerals in soils: Past, present and future perspectives. *Clay Miner.*, 34, 7–25.